ENGINEERING CASE LIBRARY

ECL - 283

FRACTURE MECHANICS AND HELICOPTER FAILURE

On October 23, 1985 a helicopter crashed while on test near Edmonton, killing the two pilots on board. Diane Rocheleau is asked to investigate the fracture and failure of the rotor collective sleeve to determine if it was the cause of the helicopter accident. She would spend approximately 240 hours on the project, examining the fracture, carrying out tests, and preparing a report. Her knowledge of fracture mechanics became the clue to unravelling the mystery.

This Case was prepared by Diane Rocheleau under the direction of Professor G. Kardos as an Independent Study at Carleton University.

FRACTURE MECHANICS AND HELICOPTER FAILURE

REFERENCES

Superscripts in the text refer to the following:

1) **Deutschman, Michels and Wilson**, Machine Design, Theory and Practice, Macmillan 1975, p 894(b).

2) **Richard W. Hertzberg**, Deformation and Fracture Mechanics of Engineering Materials, 2nd edition, Wiley 1976. pp 279-289.

3) **R.C. Shah and A.S. Kobayashi**, On the Surface Flaw Problem, The Surface Crack: Physical Problems and Computational Solutions, presented at The Winter Annual Meeting of The American Society of Mechanical Engineers, New York, November 26-30, 1972.

4) **F.W. Smith and D.R. Sorensen**, Mixed Mode Stress Intensity Factors for Semielliptical Surface Cracks, Colorado State University, prepared for National Aeronautics and Space Administration, Grant NGL 06-002-063. June 1974.

5) **C. Dale Little and Philip M. Bunting**, The Surface Flaw in Aircraft Structures and Related Fracture Mechanics Analysis Problems, Convair Aerospace Division, General Dynamics, Forth Worth, Texas. The Surface Crack: Physical Problems and Computational Solutions, presented at The Winter Annual Meeting of The American Society of Mechanical Engineers, New York, November 26-30, 1972.

6) **Campbell, Gerberich and Underwood**, Application of Fracture Mechanics for Selection of Metallic Structural Materials, Published by American Society for Metals, 1982.

7) **Battelle Institute**, Aerospace Structural Metals Handbook, Volume i, 4340 steel.

8) **Battelle**, Structural Alloys Handbook, Columbus Laboratories, 4340 steel.

9) **J.P. Gallagher and R.P. Wei**, Corrosion Fatigue Crack Propagation Behaviour in Steels., page 411.

10) **W.W. Gerberich and Y.T. Chen**, Hydrogen-Controlled Cracking - An Approach to Threshold Stress Intensity, Metallurgical Transactions A, Volume 6a, February 1975, pp 271-278.

11) **D.P. Rooke and D.J. Cartwright**, Compendium of Stress Intensity Factors, Discs, tubes and bars. pp 237-238. Flat sheets. pp 140-141.

FRACTURE MECHANICS AND HELICOPTER FAILURE (A)

THE HELICOPTER CRASH

Diane Rocheleau graduated in 1982, with a degree in Mechanical Engineering from Carleton University in Ottawa. Since graduation, she worked in the field of failure analysis and accident investigation for the Transportation Safety Board of Canada (TSBC) the federal department responsible for carrying out aircraft, marine, rail and pipeline accident investigations. She found this type of work very challenging due to the unique nature of each problem. Because of her interest, she was looked on as the resident expert in Fracture Mechanics. A helicopter accident in Edmonton presented her with a problem on which she would spend 240 hours.

Throughout the project she examined the fractures, carried out the tests, searched the literature, carried out numerous the fracture mechanics calculations, and finally wrote a report on her findings. During the project, she consulted with Professor Kardos, from whom she had taken undergraduate and graduate courses in Mechanical Design and Fracture Mechanics at Carleton University. Her final report was completed in September 1986.

She describes the project as follows.

On October 23, 1985, while attending a non-destructive testing course in Calgary, I heard that a Bell 214ST had crashed near Edmonton, fatally injuring the two pilots on board.

When I returned to work three days later, the wreckage was laid out in the main bay of our lab in Ottawa. Jim Hutchinson, who was then in charge of the Failure Analysis section, explained the situation. He had examined the collective sleeve which, during the investigation, was found broken at the lower end. The sleeve is part of the main rotor mast assembly on the Bell 214ST helicopter. Because it controls the pitch of the main rotor blades, failure is critical. The sleeve is a hollow cylinder which moves along the main rotor mast (Exhibits 1 and 2).

Jim had already examined the fracture with a binocular microscope with Ken Pickwick who is in charge of the Scanning Electron Microscope (SEM) section. The fracture features were consistent with a hydrogen assisted cracking. Because of the extent of the SEM work required, Ken would write the report on the collective sleeve failure.

I examined the fracture in the microscope; there were over 200 fisheye precracks along the outer circumference of the sleeve. Fatigue could be seen starting from some of those precracks. The precracks had a shiny appearance, typical of an intergranular mode of failure, and consistent with a hydrogen assisted failure (Exhibit 3).

On October 31st, Jim and I discussed the sleeve failure in Ken's office. Jim said that

the aircraft had broken up in-flight. This was based on the wreckage scatter pattern and eye witness statements. Ken had already contacted Bell Helicopter Textron (BHT) to discuss the failure and to obtain data on the sleeve loading. BHT told Ken that they would provide the data, but that the loading was not sufficient to cause an in-flight failure. Ken learned from BHT that there had been a previous sleeve failure in the Sultanate of Oman. BHT was sending us the details about the failure of this "Omanian sleeve".

The serial number of the Omanian sleeve was A19-00244, which identified it as being from the same batch as the sleeve we had from the Edmonton crash. The Omanian sleeve broke during cruise when the helicopter was going at 120 knots 500 feet above the ground. The pilot encountered a loss of , but safely landed the aircraft. The collective sleeve had fractured circumferentially after only a total of 123 hours in service.

The investigations carried out by BHT on that Omanian failure indicated that during manufacture, the inspection of the chromium plating operation was unacceptable. Reworking of the faulty batch involved removal of the chromium plating by immersion in a bath of inhibited hydrochloric acid. The sleeves were then replated, rebaked, and shipped to the aircraft manufacturer. Hydrogen from the hydrochloric acid bath had caused hydrogen embrittlement. The baking process had not been effective in removing it.

Subsequent to the first collective sleeve failure, the Federal Aviation Administration (FAA), which regulates aviation in the United States, issued Airworthiness Directive (AD) T84-05-51 on 27 February 1984 (Exhibit 4). This AD requires the inspection of all sleeves part number 214-010-411-001/003 with the serial number prefix "A19" using fluorescent magnetic particle inspection. The AD referred to the BHT Service Bulletin 214ST-84-17 for the detailed inspection procedure (Exhibit 5).

The sleeve we had was part number 214-010-411-001, and serial number A19-00236, and was subject to the inspection in the Service Bulletin. I got a copy of the Bulletin from the Bell 214ST Service Information microfiches in our laboratory.

Jim and I did some preliminary non-destructive testing on the sleeve near the fracture surface, using magnetic particle and dye-penetrant inspection. We followed the instructions in Service Bulletin 214ST-84-17. It requires the paint be stripped from the fillet radius where the failure occurred. We found numerous cracks on the exterior surface of the sleeve, next to the fillet radius (Exhibit 6). We now knew that a proper inspection of that sleeve would have revealed cracking. Ken went to get in touch with the helicopter operator.

The operator told Ken that as soon as the AD had come out, the sleeve had been inspected by operator's inspection sub-contracted . At that time the sleeve had accumulated 1197.4 hours service. No cracks were detected. However, the operator later found out that the inspection had been carried out before receiving Service Bulletin 214ST-84-17 detailing the correct preparation of the surface prior to the inspection. Consequently, the paint stripping had not been carried out. This was not of immediate concern, because the Service Bulletin

stated specific deadlines for inspection depending on the time in service of the sleeve since new. This sleeve had only accumulated 1197 hours, and for sleeves with 1000 hours or more, inspection was only required at 2500 hours. When this sleeve failed, it had accumulated only 2,039 hours, still within inspection limits.

Transport Canada - who regulates aviation in Canada - had been closely following our investigation, and discussed our findings with BHT and with the FAA. As a result, on November 8th, 1985, the FAA issued Airworthiness Directive 85-23-05, requiring an immediate and repetitive magnetic particle inspection of suspect collective sleeves (Exhibit 7).

The extent of precracking on the fracture surface had to be determined. It could not simply be measured under a microscope given the size of the fracture surface and the number of precracks (over 200). The area had to be magnified and the measurement computerized.

On November 1st, 1985, I made some photos of the sleeve, and close-ups of the fracture surface at 7.5 magnification. This was large enough to measure the size of each precrack, but not so large that we couldn't arrange the photos into a large montage. A digitizer was used to computerize the measurements, . Many of the precracks were touching each other. Since only the total area was needed, care had to be taken in entering the coordinates of the junction of contiguous precracks, and to enter several points along the contour of each precrack. The coordinates included the fatigue extension of the precracks. Lee, our Project Control Officer, did this in a couple of days.

The precracks were in the form of fisheyes which started either at or near the outer surface of the collective sleeve tube. The fisheyes penetrated up to 77 percent of the total thickness of the sleeve wall and were in a continuous pattern around the tube circumference, except for two fisheye-free zones, each approximately 3.1 inches in length (Exhibit 3). The wall thickness at the fracture location was 0.068 inch, and the outer diameter of the sleeve was 4.529 inches. From this, we established that the total precracked area was approximately 28 percent of the total load bearing area. The fatigue growth from the fisheyes was small, approximately one percent.

Next, we needed to verify the sleeve ultimate tensile strength and determine if it was embrittled, which would lower the fracture toughness.

Eight specimens were cut from the sleeve, and tested in tension to fracture. Of the eight samples, five were from the region immediately adjacent to the fracture, and three from a region remote from the fracture. The location of the fracture plane for the tensile test was about 1½ to 2 inches from the actual sleeve fracture surface for the five specimens cut in the immediate region of fracture surface. This location was considered to be within the embrittled region, since a magnetic particle inspection had revealed cracks in this area. Fisheyes were actually observed on one of the fractured tensile specimens.

The Ultimate Tensile Strength (UTS) for one sample, adjacent to the fracture area, was

138 Ksi. The UTS for the remaining seven samples ranged from 180 to 213 Ksi, for an average value of 195 Ksi. This is within the manufacturer's specified range of 180-200 Ksi. Microscopic examination showed that only the sample exhibiting the low ultimate tensile strength of 138 ksi contained fisheyes. Interestingly the 138 Ksi corresponded to a 29 percent reduction in load bearing area, the same as the extent of precracking on the failed sleeve. Hardness testing gave an average hardness of 72 Rockwell "A", equivalent UTS of 200 Ksi. These results, and the fact that fatigue growth from the fisheyes was minimal, indicated that the sleeve was not in an embrittled condition. Therefore, I took the ultimate tensile strength as the average value obtained, 195 Ksi, and estimated the yield point to be approximately 85 percent of that value.

BHT had tested coupons cut from a similar tube, where approximately 50% of the total surface area was cracked. The Ultimate Tensile Strength they obtained for the flawed tube was 150 Ksi. Their tests were carried out at a slow strain rate, in which the specimens failed in an average time of 1 hour.

The question we were now faced with was: had the sleeve broken as a result of the in-flight break-up, or was it a factor in leading to the break-up. Ken, Jim and I knew there was only one way to find out, and this was to carry out a Fracture Mechanics analysis. Jim asked me if I would do the calculations. I said "Sure, no problem, I'll get right on it".

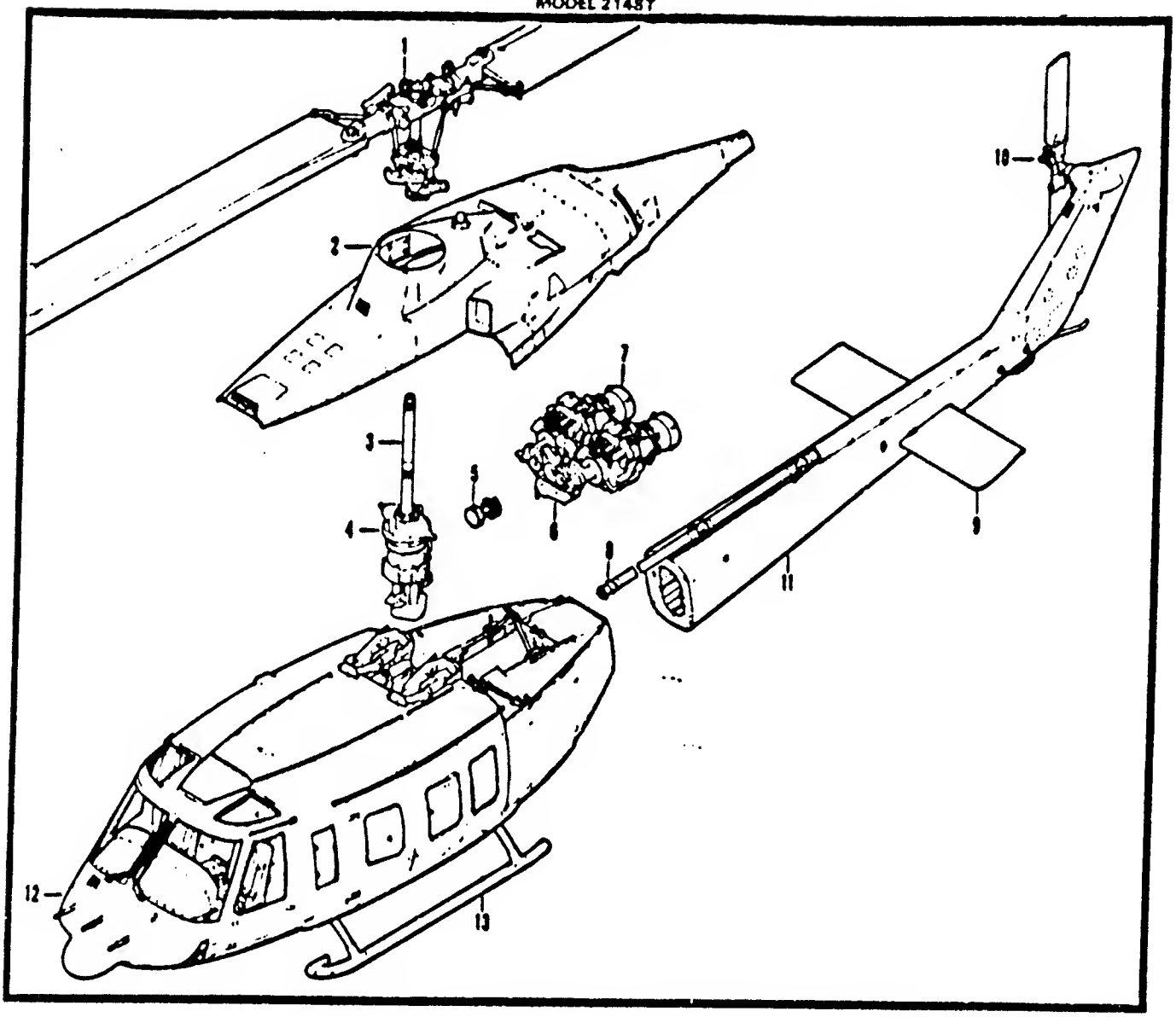

Figure 1-4. Exploded View of Model 214ST Helicopter

INDEX NUMBER	TITLE	CHAPTER
1	HUB AND BLADE INSTALLATION	62-00-00
2	COWL ASSEMBLY	71-00-00
3	MAST ASSEMBLY	62-00-00
4	TRANSMISSION ASSEMBLY	63-00-00
5	COMBINING GEARBOX TO TRANSMISSION MAIN DRIVESHAFT INSTALLATION	63-00-00
6	COMBINING GEARBOX ASSEMBLY	63-00-00
7	ENGINE ASSEMBLY	72-00-00
8	TAIL ROTOR DRIVE	65-00-00
9	ELEVATOR INSTALLATION	55-00-00
10	TAIL ROTOR INSTALLATION	64-00-00
11	TAILBOOM INSTALLATION	53-00-00
12	FORWARD FUSELAGE ASSEMBLY	53-00-00
13	LANDING GEAR ASSEMBLY	32-00-00

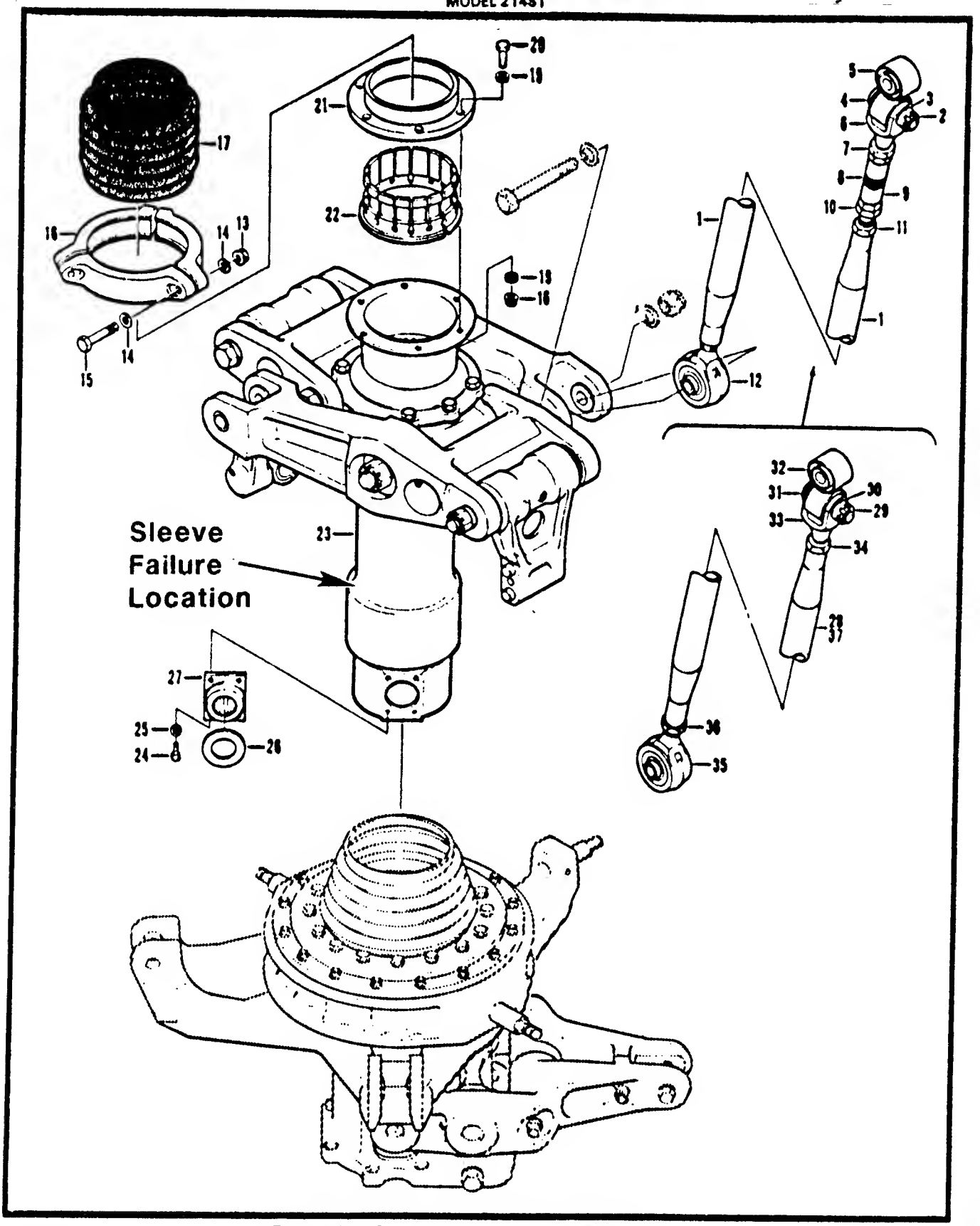

Figure 1. Controls Installation, Main Rotor

(1) FIGURE & INDEX NUMBER	(2) PART NUMBER	(3) DESCRIPTION	(4) UNIT PER ASSY	(5) NP
		SECTION: 21 ROTATING CONTROLS		
1 -	214-010-002-103	CONTROLS INSTL, MAIN ROTOR (SEE FIG. 62-21-2 FOR BALANCE OF BREAKDOWN) (S/N 28101 THRU 28148)	1	X
	214-010-002-111	CONTROLS INSTL, MAIN ROTOR (SEE FIG. 62-21-2 FOR BALANCE OF BREAKDOWN) (S/N 28181 THRU 28188)	1	X
	214-010-002-109	CONTROLS INSTL, MAIN ROTOR (SEE FIG. 62-21-2 FOR BALANCE OF BREAKDOWN) (S/N 28180 AND SUB)	1	X
- 1	214-010-410-011	.LINK ASSY, PITCH CHANGE (FAA) (S/N 28101 THRU 28152)... (REPLACED BY 214-010-410-128)	2	X
- 1	214-010-410-128	.LINK ASSY, PITCH CHANGE (REPLACES 214-010-410-011).....	2	
- 2	MS14144L10	..NUT.....	1	
- 3	140-007-41-36A3	..WASHER.....	1	
- 4	50-047-10-29	..BOLT.....	1	
- 5	214-010-434-001	..BEARING, UNIVERSAL.....	1	
- 6	214-010-485-001	..CLEVIS.....	1	
- 7	209-010-421-003	..NUT.....	1	
- 8	214-010-481-001	..DECAL, PITCH LINK.....	1	
- 9	209-010-414-001	..BARREL.....	1	
- 10	208-010-421-001	..NUT.....	1	
	214-010-410-013	..TUBE ASSY (USBL ON 214-010-410-011).....	1	X
	214-010-410-127	..TUBE ASSY (USBL ON 214-010-410-128).....	1	
- 11	209-010-413-001	...ADAPTER (USBL ON 214-010-410-013).....	1	
- 11	209-010-413-103	...ADAPTER (USBL ON 214-010-410-127).....	1	
- 12	214-010-435-003	...BEARING, ROD END.....	1	
- 13	MS21042L5	.NUT.....	3	
- 14	AN960C516	.WASHER.....	6	
- 15	AN5-15A	.BOLT.....	3	
- 16	214-010-483-001	.SEGMENT, CLAMP.....	3	
- 17	214-010-462-105	.BOOT.....	1	
- 18	MS21042L4	.NUT.....	8	
- 19	AN960C416	.WASHER.....	12	
- 20	NAS1304-8	.BOLT.....	6	
- 21	214-010-414-001	.RING CLAMP, COLLECTIVE FRICTION COLLET (NOTE 1).....	1	
- 21	214-010-414-105	.RING CLAMP, COLLECTIVE FRICTION COLLET (NOTE 1).....	1	
- 22	214-010-436-001	.COLLET SET, MATCHED (NOTE 1).....	1	
- 22	214-310-402-101	.COLLET SET, MATCHED (NOTE 1).....	1	
- 23	214-010-501-103	.SCISSORS AND SLEEVE ASSY (SEE FIG. 62-21-3 FOR DETAIL.. BREAKDOWN) (S/N 28101 THRU 28150) (REPLACED BY 214-010-501-107)	1	
- 23	214-010-501-107	.SCISSORS AND SLEEVE ASSY (SEE FIG. 62-21-3 FOR DETAIL.. BREAKDOWN) (S/N 28151 THRU 28158) (REPLACES 214-010-501-103)	1	
- 23	214-010-501-105	.SCISSORS AND SLEEVE ASSY (SEE FIG. 62-21-3 FOR DETAIL.. BREAKDOWN) (S/N 28151 THRU 28189) (REPLACED BY 214-010-501-113)	1	
- 23	214-010-501-113	.SCISSORS AND SLEEVE ASSY (SEE FIG. 62-21-3 FOR DETAIL.. BREAKDOWN) (REPLACES 214-010-501-105)	1	
- 24	214-010-864-101	.BOLT.....	8	
- 25	140-007-19S14A3	.WASHER.....	8	
- 26	214-010-464-003	.WASHER, THRUST.....	2	
- 27	214-010-460-105	.BEARING ASSY.....	2	
- 28	214-010-490-103	.LINK ASSY, PITCH CHANGE (CAA).....	2	
- 29	MS14144L10	..NUT.....	1	
- 30	140-007-41-36A3	..WASHER.....	1	
- 31	50-047-10-28	..BOLT.....	1	
- 32	214-010-434-001	..BEARING.....	1	
- 33	214-010-485-001	..CLEVIS.....	1	
- 34	208-010-421-003	..NUT.....	1	
- 35	214-010-435-003	..BEARING.....	1	
- 36	AN316C14	..NUT.....	1	
- 37	214-010-490-115	..TUBE ASSY.....	1	
		NOTE 1. USE 214-010-414-105 AND 214-310-402-101 AS A UNIT FOR SPARE PART REPLACEMENT OF 214-010-414-001 AND 214-010-436-001.		

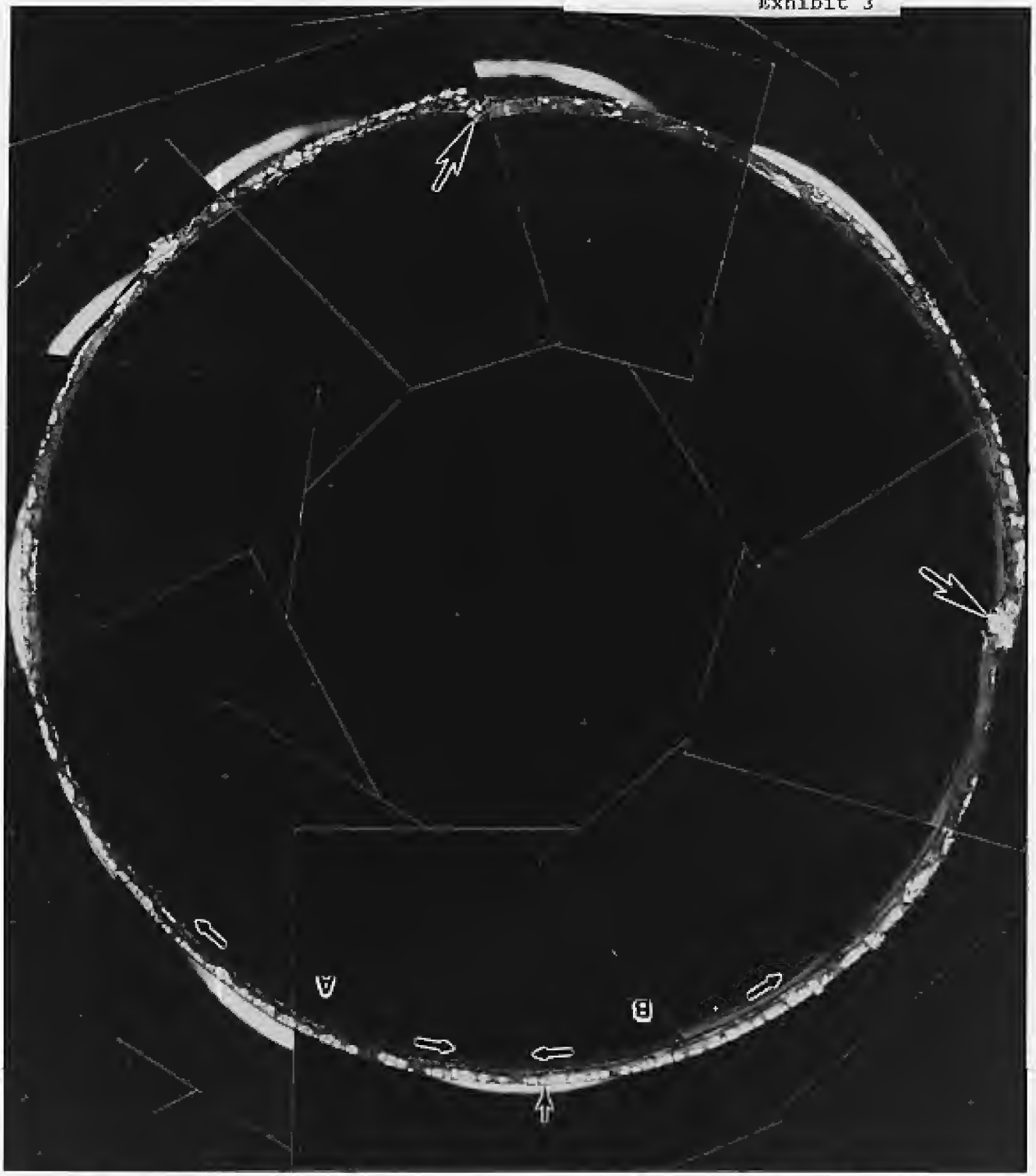

EXHIBIT 3 - MONTAGE OF THE FRACTURE SURFACE ON THE SLEEVE SHOWING THE HYDROGEN EMBRITTLEMENT PRECRACKS (FISHEYES). ARROWS POINT TO AREAS OF INTEREST.

T84-05-51 BELL HELICOPTER TEXTRON INCORPORATED:

Telegram issued February 27, 1984. Applies to Bell Helicopter Textron, Incorporated, Models 214B, 214B-1, and 214ST helicopters certified in all categories that are equipped with collective sleeves P/N 214-010-411-(all dash numbers) that have the serial number prefix A-19. (Airworthiness Docket No. 84-ASW-11.)

Compliance is required as indicated.

A. The affected parts shall be magnetic particle inspected using the procedures described in Bell Helicopter Textron, Incorporated, Telegraphic Alert Service Bulletin No. 214ST-84-17 or 214B-84-26, as applicable, or other FAA approved equivalent procedure, in accordance with the following schedule:

1. For those parts in the range of zero to five hundred hours time-in-service, perform the inspection before further flight.

2. For those parts in the range of 500 to 1000 hours time-in-service, perform the inspection prior to the next 100 hours time-in-service.

3. For those parts that have 1000 or more hours in service, perform the inspection not later than the next 2500 hour overhaul period already required by the manufacturer.

B. Remove any cracked part from service and replace it with a serviceable part.

C. The helicopter may be flown to a repair base for the above inspections under the provisions of FAR 21.197.

D. Any equivalent means of compliance with this AD must be approved by the Manager, Helicopter Certification Branch, Federal Aviation Administration, Southwest Region.

E. Bell Helicopter Textron, Incorporated, Telegraphic Alert Service Bulletin 214ST-84-17, or 214B-84-26 is equivalent means of compliance with this AD.

This AD becomes effective upon receipt.

ECL-283 (A)
Exhibit 5

ALERT SERVICE BULLETIN NO. 214ST-84-17

Bell Helicopter Textron

A subsidiary of Textron Inc.

Post Office Box 482 • Fort Worth, Texas 76101

DATE	DATE - 3-12-84
REV.	PAGE NO. 1 of 7

MODEL AFFECTED: 214ST

SUBJECT: COLLECTIVE SLEEVE, P/N 214-010-411-001, WITH SERIAL NUMBER A-19 PREFIX, INSPECTION OF

HELICOPTERS AFFECTED: S/N'S 28101 28103 through 28127 and spares shipped before 24 February 1984.
(S/N's 28102, 28128 and subsequent and spares shipped after 24 February 1984 will be complied with).

COMPLIANCE:

- Collective sleeve with less than 500 flight hours shall be inspected immediately per the accomplishment instructions (a ferry flight to a maintenance base is authorized).
- Collective sleeve with 500 hours or more but less than 1000 flight hours shall be inspected within the next 100 flight hours per the accomplishment instructions.
- Collective sleeve with 1000 flight hours or more required no inspection per this bulletion.

This Alert Service Bulletin is the formal transmital of telegraphic Alert Service Bulletin 214ST-84-17, dated 24 February 1984, with changes and additions.

EXHIBIT 5
Page 1 of 7

Test 05197 Rev. 1278

AN APPROPRIATE ENTRY SHOULD BE MADE IN THE AIRCRAFT LOG BOOK UPON ACCOMPLISHMENT
IF OWNERSHIP OF AIRCRAFT HAS CHANGED PLEASE FORWARD TO NEW OWNER

A.S.B. 214ST-84-17
Page 2 of 7

DESCRIPTION:

A 214ST in cruise flight at 120 knots and 500 ft. AGL encountered a loss of collective control. The helicopter was landed safely with no injuries but did incur some damage. The pilot reported a sudden drop of torque to approximately 30 percent. It was determined that the collective sleeve, P/N 214-010-411-001 had fractured circumferentially. The part S/N A19-00244, had approximately 123 hours.

BHTI has examined the fractured part and determined the cause to be hydrogen embrittlement.

This is the only known field problem with this part number which is also utilized on Models 214A/B/C helicopters.

During manufacture, surface cracks were found on part serial number A19-00244. BHTI records show that the cracks were removed and part subsequently accepted. Initial re-examination of BHTI spares stock revealed one zero time part with A-19 serial number prefix had micro-cracking also due to hydrogen embrittlement. This part has also been reworked on the same report and for the same reason as part S/N A19-00244. During re-examination of additional parts of BHTI production stock two additional A19 prefixed part with micro-cracking was found. This part number 214-010-411-001 has been manufactued by several sources, however, only parts with A-19 serial number prefix require inspection by this bulletin. All the other manufactuers' sleeves have an "R" as the first letter of the serial number prefix.

FAA APPROVAL:

Not required

MANPOWER:

Man-hours are based on "hands-on" time. Elapsed time to accomplish the required task may vary due to manpower and facilities available. It is estimated that eight (8) man-hours will be required to accomplish this bulletin.

MATERIALS:

The following list of materials may be required to accomplish this bulletin and may be ordered from your local BHTI Supply Outlet:

Part Number	Nomenclature	Quantity
T101709	Wrench	1 ea.
*T1013213-105	Shoe	1 ea.

*Part of kit, P/N T103213-101, for mast wear sleeve removal. (If not available, see ACCOMPLISHMENT INSTRUCTIONS Step 9).

WEIGHT AND BALANCE:

Not affected

ELECTRICAL LOAD DATA:

Not affected

REFERENCES:

214ST Maintenance Manual Chapters 62-01-00, 62-21-00 and 20-30-00.
214ST Component Repair and Overhaul Manual, Chapter 62-21-05 and 62-21-09.

PUBLICATIONS AFFECTED:

Not affected

ACCOMPLISHMENT INSTRUCTIONS:

1. Remove main rotor hub and blade assembly, and pitch links in accordance with the Maintenance Manual, Chapter 62-01-00. Using the Maintenance and Component Repair and Overhaul Manual as a guide, disassemble/remove only parts required to remove collective sleeve.

2. Remove friction collet boot, friction collet clamp set, ring clamp and collet set per Maintenance Manual, Chapter 62-01-00.

Refer to Component Repair and Overhaul Manual Chapter 62-21-09 for Steps 3 through 5.

3. Place a reference mark on drive plate and hub. Remove drive plate.

A.S.B. 214ST-84-17
Page 4 of 7

CAUTION

UPPER COLLECTIVE SLEEVE NUT HAS LEFT HAND THREADS.

4. Remove upper collective sleeve nut lock pin and loosen nut using T101709 wrench.

5. Remove scissors to hub pivot bolts and carefully swing scissors assemblies outward.

CAUTION

PROTECT SCISSORS, DRIVE LINKS ASSOCIATED PARTS FROM DAMAGE.

6. Remove collective levers (refer to Chapter 62-22-05 of Component Repair and Overhaul Manual).

7. Remove collective sleeve bearing housings (Refer to Chapter 62-21-00 of Maintenance Manual).

8. Carefully lift collective sleeve and scissors hub off mast.

9. Remove upper collective sleeve nut and press sleeve from scissors hub using an appropriate pressing tool.

NOTE

If T103213 shoe is not available, a pressing tool of an outside diameter of approximately 4.625 inches may be fabricated. The outside diameter of the sleeve at bearing area is 4.7490 to 4.7496 inches.

10. Prepare part for magnetic particle inspection by removing the paint and primer in an area approximately 3 inches above the chrome plating. Use of any of the MIL-R-81294 alkaline type strippers is acceptable for removal of the epoxy polyamide primer. This will minimize the effort required to remove the primer.

CAUTION

DO NOT USE ANY OF THE ACID TYPE ACID TYPE REMOVERS. DO NOT REMOVE THE CADMIUM PLATING.

NOTE

Inspect the sleeve by magnetic particle using the following procedures. The formula used for determining amperage (meter) is ampere turns equals number of coil turns (on coil name plate) multiplied by amperage (meter).

Example: For a 5 turn coil, 20,000 ampere turns divided by 5 coil turns equals 4,000 amperes.

NOTE

The above formula is for direct current (DC) however, if alternating current (AC) magnetic particle inspection equipment is used, use 60 percent of DC amperes specified.

11. Place a two inch diameter or larger central conductor (copper or aluminum bar) which is at least 2 inches longer than the sleeve through the longitudinal axis of the sleeve. Place the central conductor between the contact heads of the inspection equipment. Apply a gentle flow of suspension to the part outside diameter. Using 3700 to 4000 amperes, close the switch three times in quick succession while flowing the suspension. Rotate sleeve 120 degrees and remagnetize. Allow the part to dwell five minutes without disturbing the suspension film of the outside diameter.

12. Inspect visually for indications. Pay particular attention to the cadmium plated radius next to the chrome plated diameter, and the three inch wide zone above this radius. The radius is approximately 6-3/4 inches above the lower end of the sleeve. In addition, utilizing 10X magnification, examine the area of the radius tangency and include the zone to one inch above. Use white light (not fluorescent) for this inspection. Any indication is cause for part rejection.

13. After the central conductor (head) shot has been completed, perform coil shot using the following procedures:

a. Locate coil such that the longitudinal axis of the sleeve is perpendicular to plane of coil with the lower end of the sleeve protruding about 5 inches from the end of the coil. Magnetize the sleeve using 17,000 to 20,000 ampere-turns.

b. Inspect as previously described in Step 12, including the use of 10X magnification. Any indication is cause for rejection.

NOTE

Rejected sleeve shall be returned to BHTI,Trinity and Norwood, Fort Worth, Texas 76101, Attn: CPR Monitor.

14. Upon completion of the inspection demagnitize the sleeve and reprime using polyamide epoxy primer and paint as required per the Maintenance Manual, Chapter 20-30-00.

15. Carefully align scissors hub over collective sleeve and press hub onto sleeve until seated.

16. Install collective sleeve nut finger tight.

17. Install collective sleeve and scissors hub over mast.

18. Install collective sleeve bearing housings per Maintenance Manual, Chapter 62-21-00.

19. Install collective levers per Chapter 62-22-09.

CAUTION

UPPER SLEEVE NUT HAS LEFT HAND THREADS.

20. Torque collective sleeve nut 350 to 450 foot-pounds using T101709 wrench with torque wrench adapter hole. Install lock and pin safety.

For steps 21 through 23 refer to Chapter 62-21-09 of the Component Repair and Overhaul Manual).

21. Carefully swing scissors assembly onto hub and install pivot bolts.

22. Reinstall drive plate to scissors hub while aligning reference mark from Step 3.

23. Reinstall collet set, ring clamp, friction clamp set and boot per the Maintenance Manual, Chapter 62-21-00.

24. Reinstall pitch links and hub and blade assembly per Chapter 62-01-00.

25. Record bulletin compliance in Helicopter Historical Service Record (Form 7861-59020).

Please notify BHTI Product Support Department immediately of serial number checked and of findings, telephone (817) 280-3505, telex 75-8323, or 75-8304.

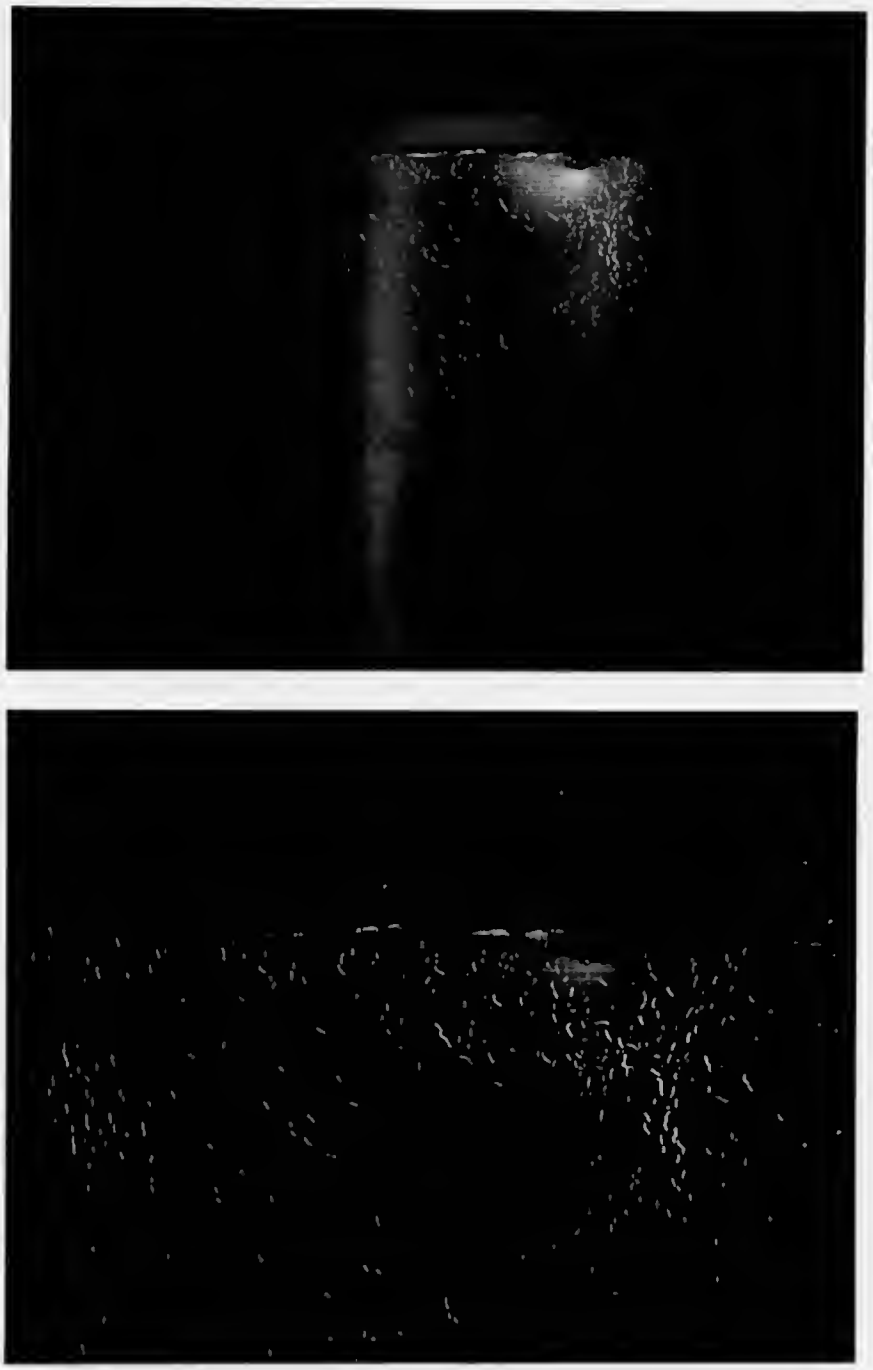

EXHIBIT 6 - ULTRAVIOLET LIGHT PHOTOGRAPHS SHOWING THE INDICATIONS OBSERVED WITH THE MAGNETIC PARTICLE INSPECTION TEST. TOP PHOTOGRAPH SHOWS THE SLEEVE AND BOTTOM PHOTOGRAPH A CLOSE-UP.

85-23-05 **BELL HELICOPTER TEXTRON, INC.:** Letter issued November 8, 1985. Applies to all Bell Helicopter Model 214B and 214ST series helicopters certified in all categories that have collective sleeve part number 214-010-411-001 or -003 with serial number AI9-00001 through AI9-00738 or serial number A-1 through A-10 installed.

Compliance is required before further flight after receipt of this AD, unless previously accomplished, and thereafter at 250 hour intervals.

To prevent failure of the collective sleeve, accomplish the following:

a. Before further flight after receipt of this priority letter AD, perform a magnetic particle inspection of the affected sleeves using the procedures described in Bell Alert Service Bulletin 214-84-26, dated March 12, 1984, or 214ST-84-17, dated March 12, 1984, as appropriate.

NOTE: It is essential that the paint and primer be removed as described in the service bulletins prior to performing the magnetic particle inspection.

b. Repeat the magnetic particle inspection every 250 hours time in service.

c. If cracks are found, replace with serviceable parts.

d. An alternative means of compliance or adjustment of the compliance time, which provides an equivalent level of safety, must be approved by the Manager, Helicopter Certification Branch, Aircraft Certification Division, FAA, Southwest Region.

This airworthiness directive is effective upon receipt.

EXHIBIT 7

FRACTURE MECHANICS AND HELICOPTER FAILURE (B)

FINDING A "BALL-PARK" FIGURE

Most of the Fracture Mechanics calculations I had carried out since graduation involved semicircular corner cracks in the bore of a hole, under plane strain conditions.

Although the problem was not the same, I thought I could get a ball-park figure of the critical flaw size and compare it to the deepest flaw size on the sleeve. Since the flaws were of a semicircular/semielliptical nature, I could use the formula:

$$K = Y \sigma \sqrt{(\pi a/Q)}$$

The stress levels supplied by BHT had been obtained using strain gauges during flight tests:

Pull-up collective mode:

$$7617 \pm 6513 \text{ psi}$$

Cruise level flight loads:

$$5524 \pm 5468 \text{ psi}$$

At the time of the in-flight break-up, the helicopter was in pull-up collective mode.

Additional factors had to be considered to determine the actual stress. The fracture occurred in a fillet, at a change of cross-section (Exhibits 8 and 9). The stress concentration factor was taken from a Machine Design textbook (Exhibit 10). The sleeve was precracked approximately 28 percent of the total load bearing area, increasing the stress at that location.

Fracture toughness depends on the material, its heat treatment, the thickness of the specimen (i.e., plane stress or plane strain conditions), and on environmental conditions. An energy dispersive x-ray analysis confirmed that the material was AISI 4340, as specified by the manufacturer .

The fracture toughness could not be calculated directly from the plastic zone size on our sleeve, as the fracture features were almost 100% slant/shear type (Exhibit 11), typical of 100% plane stress conditions, and therefore, flat areas from which I could have extracted the plastic zone size "r" were almost non existent.

$$r = (K / \sigma_y)^2 \; 1/(2\pi)$$

The sleeve had been tempered at 800°F for a period of four hours. From the "Structural Alloys Handbook" by Battelle, for a 400°F and 600°F temper, I obtained a graph of the fracture toughness versus specimen thickness for AISI 4340 (Exhibit 12). For a wall thickness of 0.068 inch, I obtained a fracture toughness value of 175 Ksi √inch. The plane strain fracture toughness from the same graph was 80 Ksi √inch. The tensile testing we carried out indicated that the sleeve was not embrittled, and thus, the data from the graph in the "Structural Handbook" was valid for the calculations.

I calculated what the size of the plastic zone size would have been using the plane strain and plane stress fracture toughness values, i.e., 80 Ksi √inch, and 175 Ksi √inch. I compared these to the sleeve wall thickness. The calculations are shown in Exhibit 13.

By applying the ASTM plane strain criteria formula, I confirmed that I had a plane stress condition:

$$\text{wall thickness} / (K_{IC} / \sigma_y)^2 \geq 2.5$$

where σ_y is the yield strength. The calculations are shown in Exhibit 14.

To verify how accurate the fracture toughness values of 80 and 175 ksi √inch were, I could use the data from the Osmian sleeve failure. The only details available to us on this failure were those written on the sketch sent to us by BHT (Exhibit 15). No other information such as the appearance of the fracture surface was available.I assumed that Cruise flight loads were applied to the sleeve and that the sleeve failed at the fillet radius approximately the same location as the Edmonton helicopter.

Only about 80 degrees of the sleeve was intact, the remainder was cracked completely through the thickness. Fisheyes were present on the remaining 80 degrees. Precise information about the depth, width and area of the fisheyes was not available. However, the figures marked on the sketch indicated that there were 12.5 fisheyes in the section still holding, the crack depths varied from 0.050 to 0.060 inches, and the crack widths from 0.080 to 0.160 inches.

Since the sleeve failed in flight while under normal operating loading conditions, we knew that the flaw size was critical. Using a crack depth of 0.050 inches, a crack width of 0.120 inches, and the number of fisheyes observed (12.5), I calculated the effective load area, and the resultant stress in cruise flight. Correcting for the change in cross-section (stress concentration factor), I obtained the actual stress. Assuming a surface flaw, I took the width of the crack as being continuous over the 12.5 fisheyes.

Calculating for fracture toughness:

$$K = Y \sigma \sqrt{(\pi a/Q)}$$

The detailed calculations are shown in Exhibit 16.

The fracture toughness value obtained was not close to the plane strain or plane stress values in the "Structural Alloys Handbook", (80 and 175 Ksi $\sqrt{inch}$, respectively), suggesting that additional correction factors had to be considered, or that the sleeve failed under conditions other than plane strain or plane stress.

Was the flaw a surface flaw or an embedded flaw ? This would affect the correction factor Y. Most of the fisheyes did not open to the surface which was cadmium plated. However, the cadmium plating layer was so thin that I considered the flaws to be surface flaws.

What were the flaw parameters ? This was not just a single crack, but rather a string of cracks, although they were not all on the same plane (Exhibit 11). The deepest crack observed around the fracture surface was 0.0525 inches, which I took as "a". I considered four possible values for the crack width "2c":

- the longest single fisheye;
- a cluster of fisheyes where the fisheyes blended into one another;
- a string of contiguous fisheyes; or
- the entire perimeter of the sleeve.

The longest single fisheye was 0.0735 inches, the longest cluster 0.1732 inches, and the longest string 1.15 inches. The perimeter of the sleeve was $2\pi r$ where r is 4.529"/2 giving a crack width "2c" of 14.23 inches. From these I could calculate the flaw shape parameter "Q" (Exhibit 17).

I now had all the data to calculate the critical flaw size for our sleeve and compare it to the deepest flaw observed. The detailed calculations can be found in Exhibit 18.

EXHIBIT 8 - COLLECTIVE SLEEVE AS-RECEIVED. THE FRACTURE IS IN THE FILLET AREA. MAGNIFICATION APPROXIMATELY 0.2 TIMES.

D = 5.12 inches
d = 4.5 inches
r = 0.5 inches

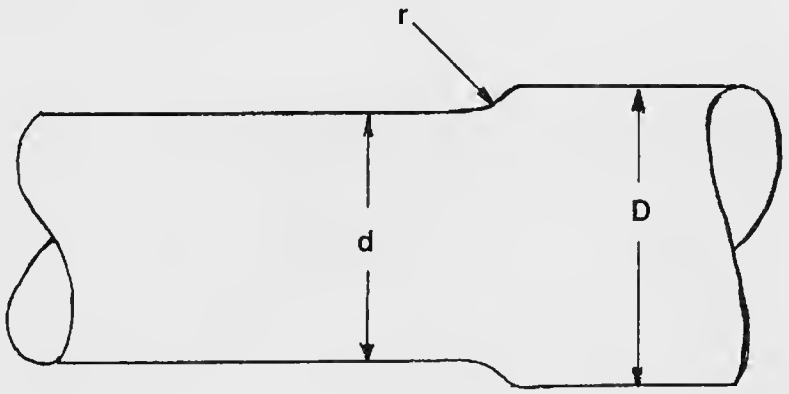

EXHIBIT 9 - SCHEMATIC OF THE COLLECTIVE SLEEVE CROSS-SECTION INDICATING THE ACTUAL DIMENSIONS. THE FRACTURE IS AT LOCATION "r".

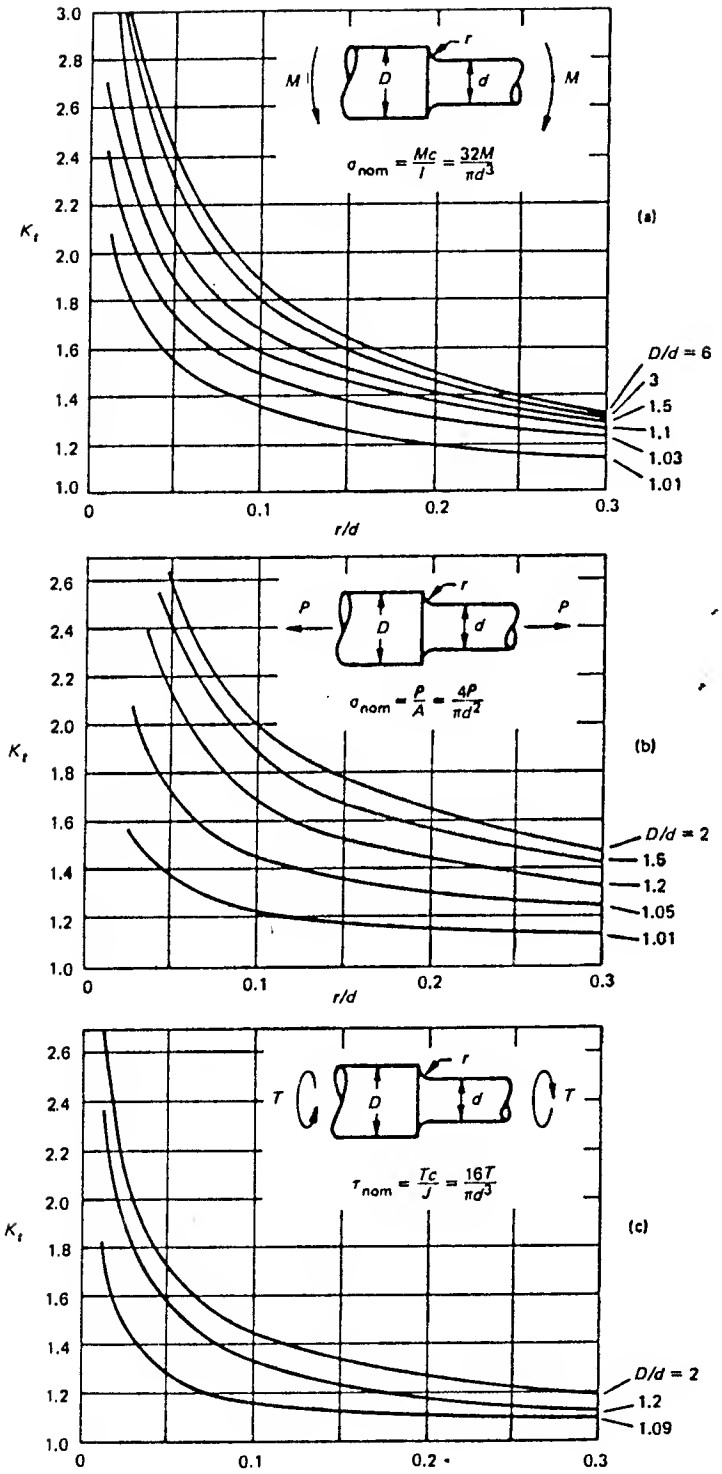

Figure B-4 Shaft with fillet (a) bending; (b) axial load; (c) torsion.

Deutschman, Michels and Wilson,
Machine Design, Theory and Practice
Macmillan 1975, page 894(b)

EXHIBIT 10

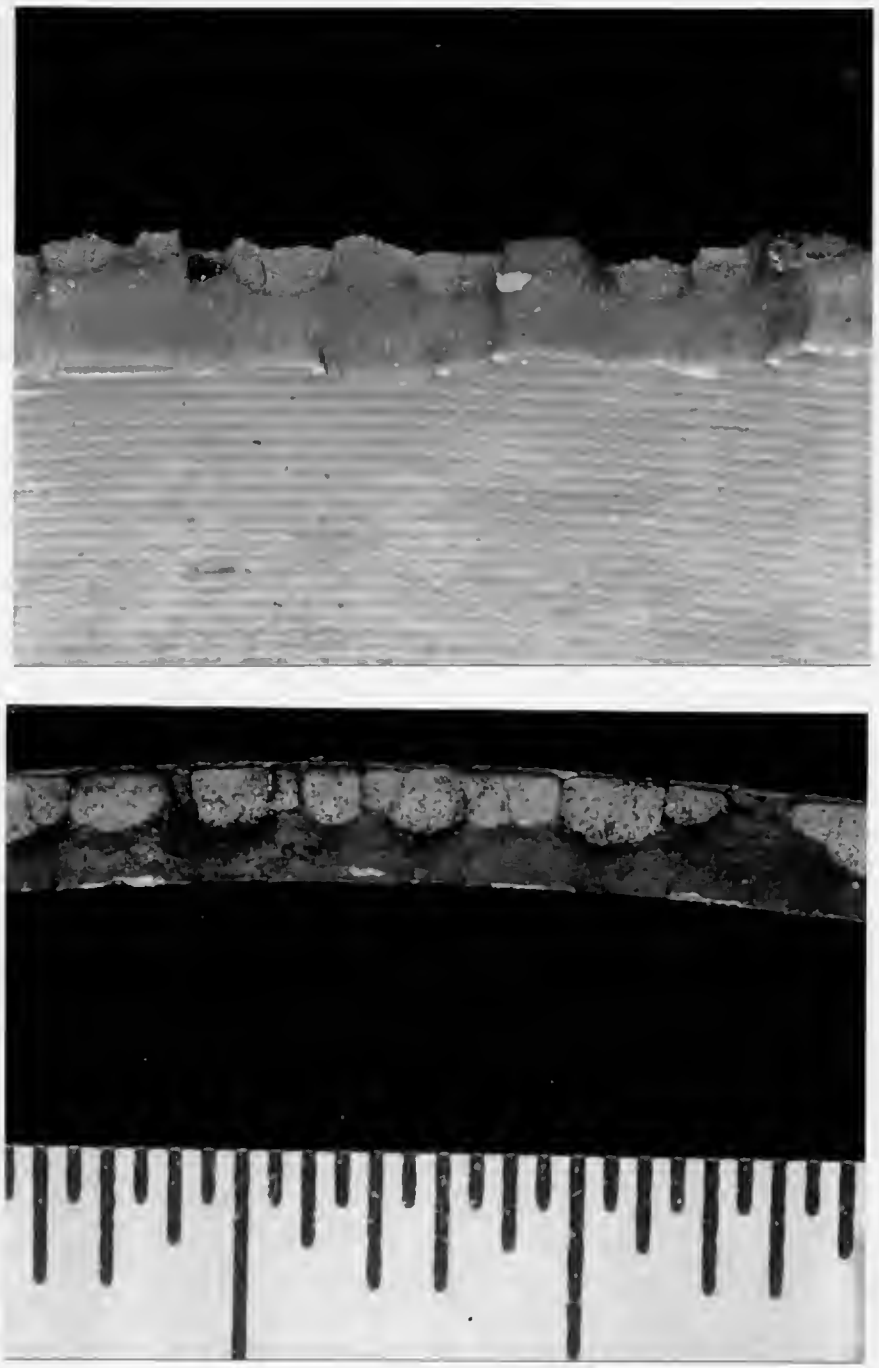

EXHIBIT 11 - CLOSE-UP OF SOME OF THE FISHEYE CRACKS. THE TOP VIEW SHOWS THE 45° SLANT OF THE FRACTURE SURFACE, AND THE DIFFERENT PLANES ON WHICH THE FISHEYES ARE LOCATED. THE BOTTOM VIEW SHOWS HOW SOME OF THE FISHEYES COLLECT IN CLUSTERS.

FRACTURE TOUGHNESS
PLANE STRAIN

4340 STEEL

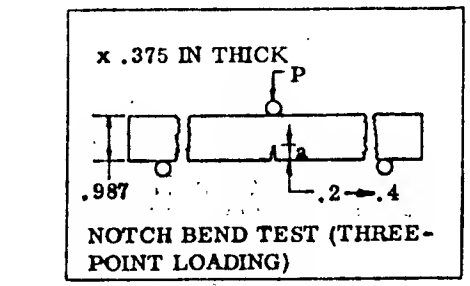

NOTCH BEND TEST (THREE-POINT LOADING)

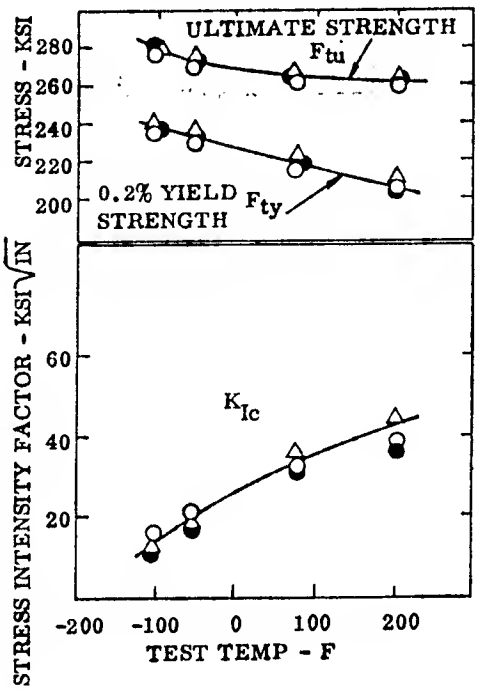

STRENGTH AND FRACTURE TOUGHNESS OF 4340 STEEL (99)

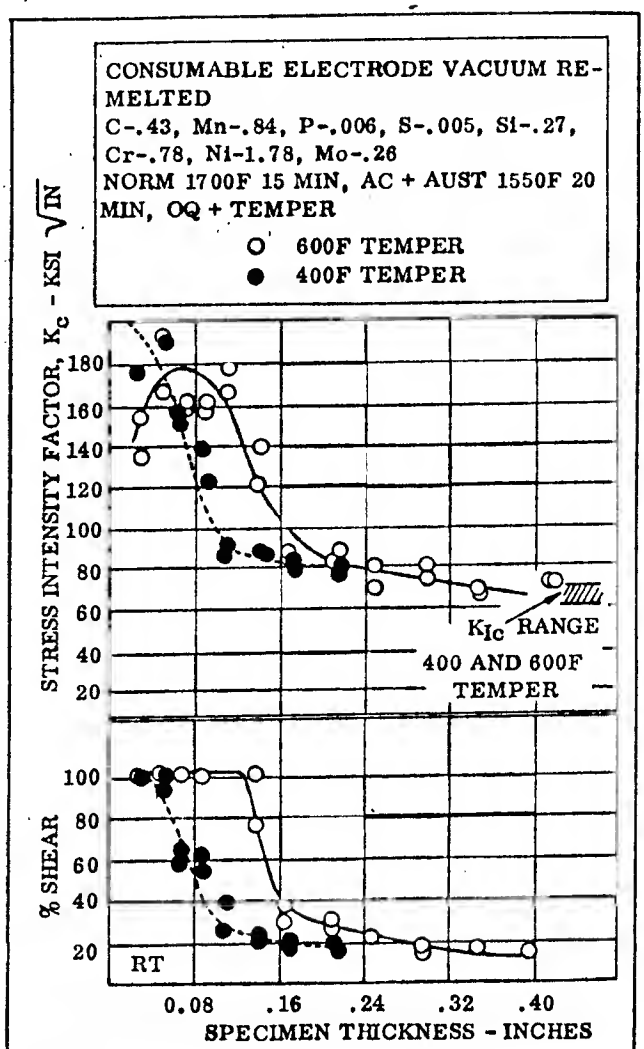

INFLUENCE OF SPECIMEN THICKNESS ON THE FRACTURE TOUGHNESS OF 4340 STEEL (122)

TENSILE AND PLANE STRAIN FRACTURE TOUGHNESS OF 4340 SHEET (100)

Strength Level (ksi)	Material Thickness (in)	Number of Specimens	F_{tu} (ksi)	F_{ty} (ksi)	e (%)	Shot Peened	Fracture Toughness K_{Ic}(a) (ksi-$\sqrt{in}$)	Fracture Toughness K_{Ic}(b) (ksi-$\sqrt{in}$)
150	.063	6	150.7	138.3	9.0	no	112	150
150	.090	5	167.6	156.2	9.6	no	127	165
150	.125	7	176.5	164.5	8.8	no	134	175
150	.063	6	166.1	151.2	7.8	yes, 110 shot	114	155
150	.063	6	157.3	137.3	8.7	yes, 330 shot	124	166
125	.063	6	136.3	124.3	12.3	no	107	146
200	.063	5	214.0	198.2	4.6	no	110	147

Longitudinal fracture toughness specimens, 7.31 in wide by 15.50 in long with 2.5 in wide center machined notch and fatigue crack.
Valid stress intensity values calculated from ASTM STP No. 381.
(a) Tensile
(b) Plane strain

EXHIBIT 12

Structural Alloys Handbook, Battelle, Columbus Laboratories 4340 ateel.

1973

EXHIBIT 13

SOLUTION : "BALL-PARK" FIGURE ON PLASTIC ZONE SIZE

Evaluate the size of the plastic zone size given plane strain and plane stress fracture toughness conditions, i.e. 80 Ksi $\sqrt{inch}$ and 175 Ksi $\sqrt{inch}$.

$r = (K/\sigma_{ys})^2 \ 1/(2\pi)$

$r = (80 \text{ Ksi } \sqrt{inch}/166 \text{ Ksi})^2 \ 1/(2\pi)$

$r = 0.037$ inch in plane strain

$r = (175 \text{ Ksi } \sqrt{inch}/166 \text{ Ksi})^2 \ 1/(2\pi)$

$r = 0.177$ inch in plane stress

In plane strain, the plastic zone size would be half the wall thickness, and in plane stress, it exceeds the wall thickness.

EXHIBIT 14

SOLUTION : "BALL-PARK" FIGURE ON PLANE STRAIN CONDITION

Determine if plane strain or plane stress conditions exist.

At the time of the in-flight break-up, the helicopter was in pull-up collective mode.

maximum stress:	7617 + 6513 = 14,130 psi
fillet stress concentration factor	$K_t = 1.6$
new stress:	14,130 psi x 1.6 = 22,608 psi
28% precracking:	22,608/0.72 = 31,400 psi

plane stress fracture toughness 175 Ksi $\sqrt{inch}$
plane strain fracture toughness 80 Ksi $\sqrt{inch}$

applying the ASTM plane strain criteria formula:

$$\text{wall thickness} / (K_{IC} / \sigma_y)^2 \geq 2.5$$

$\sigma_y = 0.85 \times 195$ Ksi = 166 Ksi
$K_{IC} = 80$ Ksi $\sqrt{inch}$
wall thickness = 0.068 inch

I get 0.29 inch which is not greater nor equal to 2.5, therefore, I have a plane stress condition.

ECL-283 (B)
Exhibit 15

Omanian Sleeve

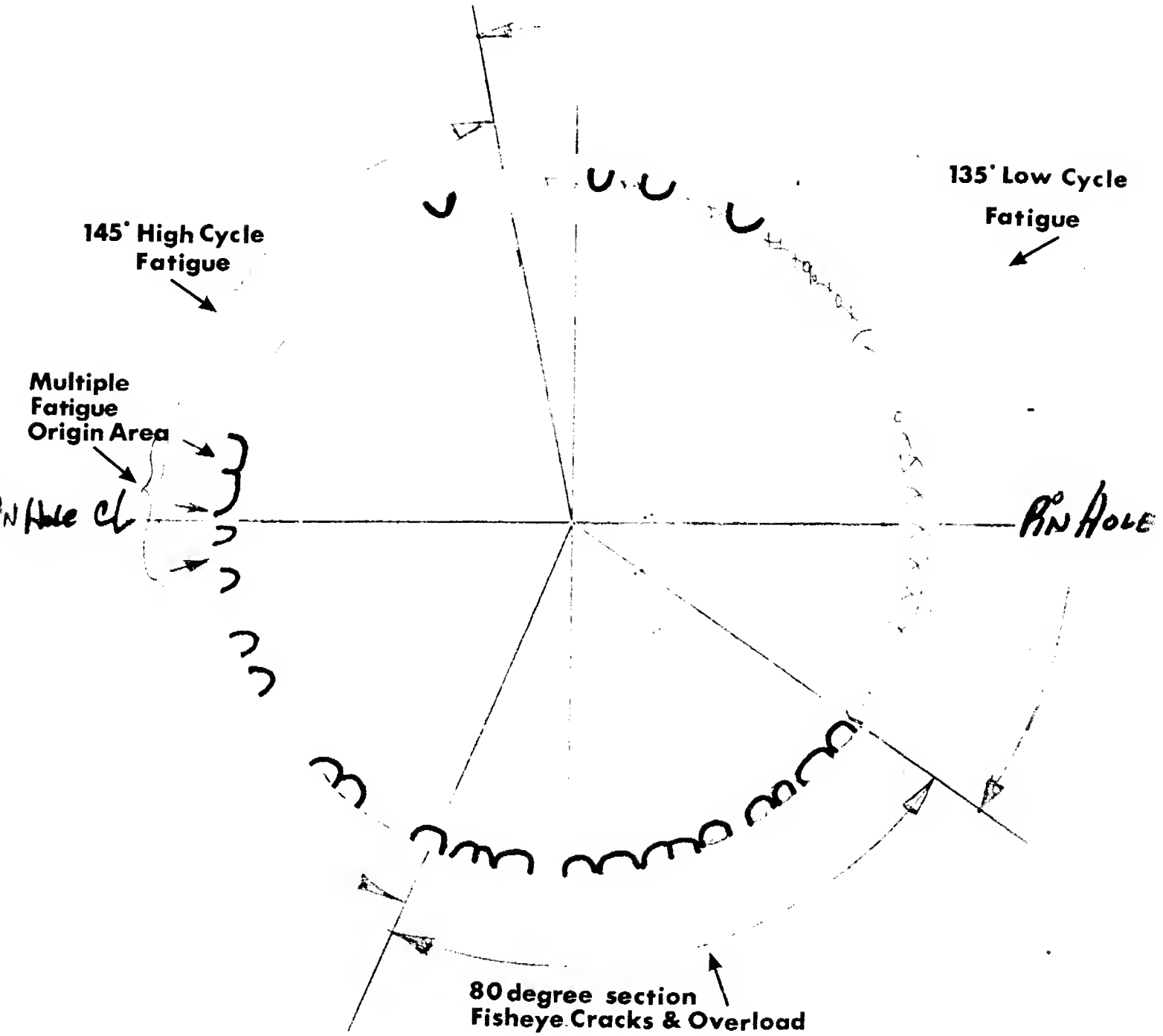

25 Fisheyes
Sleeve thickness 0.060-0.063"
Crack Width 0.080-0.160"
Crack Depth 0.050-0.060"

VIEW LOOKING DOWN AT THE FRACTURE, ON LOWER END OF THE COLLECTIVE SLEEVE

EXHIBIT 15

EXHIBIT 16

SOLUTION : "BALL-PARK" FIGURE FRACTURE TOUGHNESS ON OMANIAN SLEEVE

Determine the fracture toughness from the Omanian sleeve

The flaw size was critical since the sleeve failed in cruise flight while under normal operating loading conditions.

outer sleeve diameter = D_2 = 4.529 inches
wall thickness = 0.068 inches
inner sleeve diameter = D_1 = 4.529" - 2 (0.068") = 4.393"

original area of sleeve = $(\pi/4)\ (D_2 - D_1)^2$ = 0.953 inch^2

Area of sleeve available with 80 degree section:
80/360 x 0.953 inch^2 = 0.2118 inch^2

Depth of fisheye cracks on remaining 80 degree section:
0.050 inches to 0.060 inches. Take 0.050 inches.

Width of cracks:
0.080 inches to 0.160 inches. Take an average of 0.120"

Area of sleeve cracked, considering 12.5 fisheyes:
12.5 X 0.050 inches x 0.120 inches = 0.075 inch^2

Effective load area:
0.2118 inch^2 - 0.075 inch^2 = 0.1368 inch^2
0.1368 inch^2 / 0.953 inch^2 = 0.1435

Stress Calculation, cruise:
5524 psi + 5468 psi = 10992 psi
10,992 psi / 0.1435 = 76,599 psi
76,599 psi x 1.6 = 122,559 psi
where 1.6 is the fillet stress concentration factor

crack depth of 0.050 inches
crack width = 0.120 inches x 12.5 = 1.5 inches

σ/σ_y = 122.6 Ksi/166 Ksi = 0.74

a/2c = 0.050"/1.5" = 0.0333 gives me Q = 0.9
Y = 1.1 for a surface flaw

find K

$K = Y \sigma \sqrt{(\pi a/Q)}$
$K = 1.1 \times 122.6 \text{ Ksi } \sqrt{(\pi\ 0.050 \text{ inch} / 0.9)}$
$K = 56 \text{ Ksi } \sqrt{\text{inch}}$

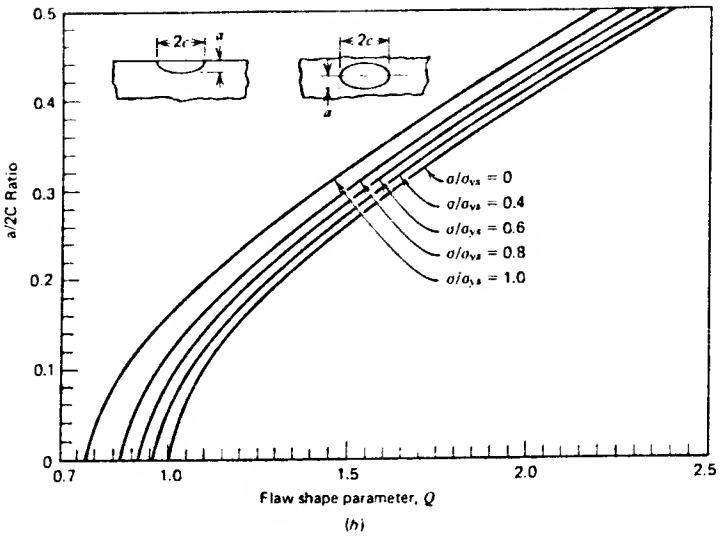

(h)

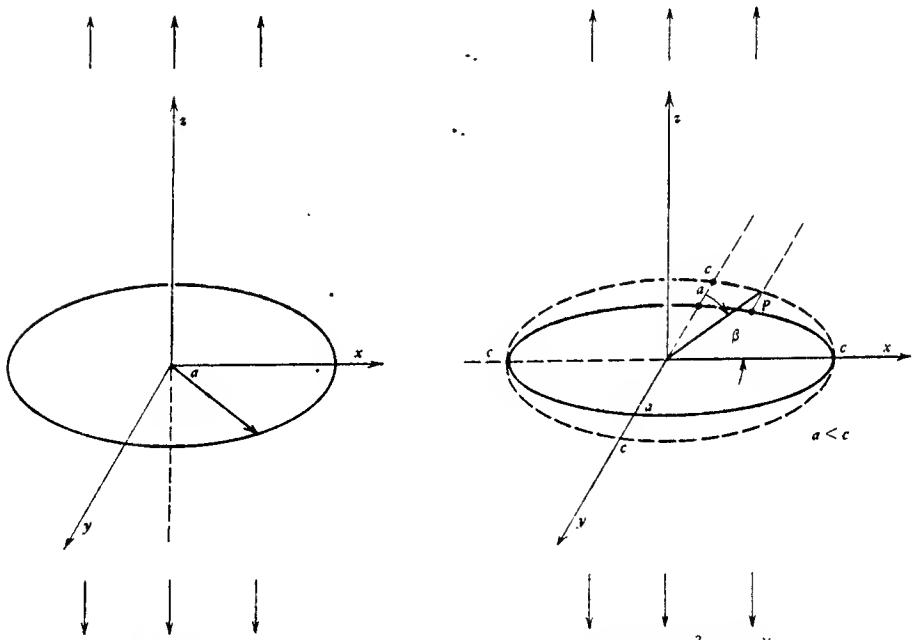

$K = Y\sigma\sqrt{a/Q}$

$Y = \sqrt{\pi}$

$Q = 2.5$

$K = \frac{2}{\pi}\sigma\sqrt{\pi a}$

(i)

$K_P = Y\sigma\sqrt{a/Q}\,(\sin^2\beta + \frac{a^2}{c^2}\cos^2\beta)^{1/4}$

$Y = \sqrt{\pi}$

(j)

FIGURE 8.7 (*Continued*)

EXHIBIT 17

Deformation and Fracture Mechanics of Engineering Materials
Richard W. Hertzberg. 2nd edition. Wiley 1976. pp 282

EXHIBIT 18

SOLUTION : "BALL-PARK" FIGURE FOR CRITICAL FLAW SIZE

Estimate the critical flaw size on our sleeve, and compare it to the deepest flaw size observed.

$$\text{"a" critical} = (K / (Y\sigma))^2 (Q/\pi)$$

Fracture toughness K: consider the three values for K:

56 Ksi √inch fracture toughness from Omanian sleeve data
80 Ksi √inch plane strain fracture toughness
175 ksi √inch plane stress fracture toughness

Y = 1.1 for a surface flaw

Flaw size "a/2c" and Q value:
"a" = 0.0525 inches
"2c" = 0.0735 inches for the longest single fisheye
"2c" = 0.1732 inches for the longest cluster
"2c" = 1.15 inches for the longest string
"2c" = 14.23 inches for the entire sleeve perimeter

Worst case calculation:

K = 56 Ksi √inch
2c = 14.23 inches
a/2c = 0.004 and Q = 1, for $\sigma/\sigma_y = 31.4 / 166 = 0.2$

$$a \text{ critical} = (K /(Y\sigma))^2 (Q/\pi)$$
a = 0.84 inches

the critical flaw size exceeded the thickness of the sleeve (0.068 inches), which meant that failure of the sleeve was a secondary event in the in-flight break-up.

FRACTURE MECHANICS AND HELICOPTER FAILURE (C)

EVENTS LEADING TO THE CRASH

When I showed the result to Jim on the 19th of November he was interested, but told me that because failure of the sleeve could have led to "mast bumping" and helicopter in-flight break-up, just a "ball-park" figure was insufficient.

I had no definite facts, but several possibilities in the choice of the flaw size, its length, its shape, the actual operating stress, the strength of the sleeve and the fracture toughness. I suspected that I had a plane stress condition, but the thickness of the sleeve wall was too small for a standard Charpy test to determine the fracture toughness experimentally.

Jim agreed that some time would have to be spent on research material before a more concrete answer could be found. He said, "Go ahead".

I then discussed the problem with Dr. Kardos at Carleton University. He suggested a few new approaches. Two days later, I initiated a library search by topic on the National Research Council CISTI computer system. I got the results the next day and selected some 30 articles from it.

Jim gave me for more details of the Edmonton accident, so that I could better understand the loading conditions involved. It was clearly established that the aircraft had broken up in-flight. What we didn't know was what initiated the break-up. The main rotor mast was bent, indicating "mast bumping". We knew that an in-flight failure of the collective sleeve could produce such an effect, but the sleeve could have failed because of the abnormal loading during mast bumping.

What is "mast bumping"? It means that a violent blade yoke to mast contact occurs. Jim showed me blade yoke impact marks on the main rotor mast. Mast bumping results from excessive main rotor blade flapping angles which may be amplified by incorrect cyclic/collective inputs. Once "mast bumping" occurs, the mast can bend, reducing the main rotor blades and tail boom clearance, allowing the main rotor blades to strike the boom.

But what causes excessive flapping blade angles ? Typically these occur during a low-g manoeuver which causes a reduction of the thrust, or unloading of the main rotor. Then, the tail rotor thrust is no longer offset by the main rotor thrust, and the aircraft rolls to the right (for helicopters in which the main rotor turns counterclockwise when viewed from the cockpit). If the pilot puts in left cyclic to counter the right roll, a normal pilot reaction, severe flapping results because the rotor is unloaded and the fuselage does not follow the rotor disk. The effect is amplified during a left turn because the moment due to fuselage weight is added to the right rolling moment of the tail rotor, resulting in larger blade flapping

angles. Correct pilot inputs of the cyclic and collective are critical to correct the problem.

How could two experienced pilots get into such a situation? The pilots were carrying out a flight to test the inverters. The inverter is an electrical device which changes direct current from the aircraft electrical supply into alternating current to operate the instruments. Essential equipment in aircraft are duplicated for redundancy, and thus there are two inverters.

The first test flight was in August 1985. It was carried out to determine what effect switching one or both inverters "off", would have on the electrical system during left and right climbing turns. For the tests, two crew members were on board. It was determined from the tests, that timely control input was critical for proper aircraft recovery. It was reported that when one inverter failed, or was switched "off", a delay occurred in transferring the load from one inverter to the other, making the aircraft less responsive to control inputs during the delay.

They also found that when both inverters failed or were selected "off", during a left climbing turn, the helicopter pitched up 10 to 14 degrees within three to four seconds. Since there is no mechanical collective to yaw coupling, the aircraft will yaw to the left if the collective is lowered quickly, producing an increasing left bank along with a nose pitch down. This would correspond to a low-g condition, and will become excessive if corrective action to counter the left yaw, is not taken within two to three seconds.

The Edmonton accident happened during the second series of tests in October 1985. The visibility in the area selected for testing was good to 15 miles, and the winds were 18 gusting to 23 knots from the ground up to 2000 feet. There was no report of turbulence other than that associated with the tree line and a lake nearby.

During the scheduled testing, at approximately 14:40 hours, witnesses observed the main rotor impact the tailboom while the aircraft was in a left turn, at 1,000 feet. The helicopter broke up in flight, crashed in a wooded area, and a fire developed. Both pilots were killed. No evidence of incapacitation or physiological problems were found during the post-mortem and toxicological examinations.

I asked Jim how fracture of the collective sleeve could result in "mast bumping". Jim told me that because the sleeve changes the pitch of the main rotor blades, its failure would allow movement of the top section independently of the collective control inputs from the cockpit. This would change the travel position of the sleeve from 46 percent in normal cruise to 26 percent, in half a second. The main rotor blades would then abruptly decrease their pitch setting, off load the rotor system, and achieve a new low blade angle. These conditions could lead to mast bumping.

Jim showed me the score marks observed on the main rotor mast, coinciding with two locations on the inner diameter of the edges of the fracture on the collective sleeve. This

indicated that the sleeve was broken when some of the score marks were made. The length of some of the marks was consistent with their having occurred during mast bending. From the score marks along the main rotor mast, it was determined that elastic mast bending occurred while the collective sleeve was in the 50 to 60 percent position. Therefore, mast bending was well under way when the collective sleeve broke, and failure of the collective sleeve did not initiate the accident sequence. Mast bending causing main rotor to tailboom strike would have supplied the over-stress necessary to break the sleeve. He added that the fracture mechanics calculation would help tie this evidence together.

FRACTURE MECHANICS AND HELICOPTER FAILURE (D)

ADDITIONAL PARAMETERS FOR IN-DEPTH CALCULATIONS

Some of the literature I had collected suggested among other things, specific fracture toughness data for environmentally stressed components and for thin sheets.

Because the parameters were not clear cut, I first made a list of the various parameters required for these calculations. These were: flaw size, flaw length, flaw shape, operating stress, fracture toughness, and a finite width correction factor. For the computations I decided to always consider the worst case condition.

From the "Compendium of Stress Intensity Factors by Rooke and Cartwright"[11] I selected two additional models for my flaw shape, and ended with three different flaw configurations:

1. a semielliptical/semicircular flaw (Exhibit 17);
2. an external/circumferential edge crack in a tube (Exhibit 19);
3. multiple collinear edge cracks in a sheet (Exhibit 20).

The opening mode stress intensity factor K_I was considered for both the circumferential edge crack in a tube and multiple collinear edge cracks in a sheet configurations.

In these three flaw shape configurations the loading is considered to be in tension as in the case for our sleeve.

The flaw shape on the Omanian sleeve was different than that on our sleeve, being more of an edge crack than a series of cracks distributed uniformly around the circumference of a tube. For Omanian case, the "multiple collinear edge cracks in a sheet" might be more applicable.

I used the same flaw depth for all cases, i.e. the deepest crack, but the length varied depending on the configuration. For the semielliptical/semicircular shape, the length was the longest fisheye string; for the external/circumferential edge crack in a tube, the length was the entire circumference; and for the collinear crack approach, the length was the average cluster size.

From the articles I found new correction factors to consider on thin sheets: the frontface correction factor, the backface correction factor, both strongly material dependent (Poisson's ratio), and the secant correction factor which is not material dependent. The thin sheet correction factor considers the stress intensity of the crack edges at the exposed surface, and is a function of the crack size, crack depth and material thickness. These correction factors were determined from articles written by Shaw and Kobayashi[3], Smith and Sorensen[4],

and Little and Bunting[5] (Exhibit 21). Some authors consider the frontface and backface correction factors independently, while others take into account their interaction. The interaction effect between the front and back face is more important for slender cracks, i.e. a small a/2c ratio as in our case. None was mentioned for AISI 4340 steel, so I chose one from a comparable type steel, and got M_k equal to 2.9. The secant correction factor approach[2] evaluates the ratio of the crack depth to twice the thickness of the material. The secant correction factor M_k for thin sheets was equal to 1.69. I considered both factors in my calculations in order to be able to compare them.

To deal with the finite width correction factors I inserted the new correction factor M_k in the formula:

$$K = M_k\ Y\ \sigma\ \sqrt{(\pi a/Q)}$$

Environmental factors and material characteristics such as UTS, tempering temperature and thickness, were considered in the evaluation of the fracture toughness and stress intensity threshold data. As the tempering temperature is increased, the UTS value will decrease, but the fracture toughness and the environmental threshold will increase. The fracture toughness data I had obtained for AISI 4340, in the "Structural Alloys Handbook" by Battelle[8], for a 400 and 600°F temper, was respectively 80 and 175 Ksi √inch data for plane strain and plane stress conditions (Exhibit 12). Since our sleeve had been tempered at a higher temperature, i.e., 800°F for a period of four hours, the fracture toughness obtained from the graph was considered to be on the conservative side.

From the literature, I obtained fracture toughness data for plane strain, plane stress, environmental threshold values for stress corrosion cracking, and the threshold values for thin sheets cracking (Exhibit 22). These values were respectively 80, 175, 26 and 35 Ksi √inch. The thickness criteria for plane stress was met for our sleeve, and the fracture features were predominantly slant (shear type), which is also consistent with plane stress conditions. However, very thin specimens could actually experience plane strain conditions if the yield strength is very high, since the plastic zone size is dependent on the yield strength of the material.[2]

Thin sheets threshold values of stress intensity K_{th}, had been found by Gerberich and Chen[10] who did a study of growth rate on different thicknesses of AISI 4340 . They found that at a stress intensity of 29 Ksi √inch on 0.75 inch thick samples, the fracture growth rate was 400 times faster than on 0.15 inch thick samples loaded to a stress intensity of 37 Ksi √inch. The threshold value of stress intensity was also observed to drastically increase when plane stress conditions were approached, i.e., when the plastic zone size "r_y" approached the thickness of the material, and in theory, could be infinite under 100% plane stress condition, i.e. the specimen would never fail.

The threshold stress intensity K_{ISCC} is the value of stress intensity below which no cracking will occur under hydrogen-assisted cracking, such as hydrogen embrittlement and

stress corrosion cracking. [9]

I had now narrowed down my parameters to:

- three different flaw configurations;
- the same flaw depth for all cases, i.e. the deepest crack;
- a frontface/backface or secant correction factor, to consider edge effects on thin sheets;
- four fracture toughness conditions data: plane strain, plane stress, environmental threshold value for stress corrosion cracking, and the threshold value for thin sheets cracking.

For each of my three flaw configurations I could now vary the different correction factors and fracture toughness data and evaluate the results. I wanted to determine for which fracture toughness data the flaw size "a" was critical, then evaluate if the sleeve was operated under these conditions.

External circumferential crack in a tube: uniform uniaxial tensile stress or uniform axial torque

A long tube, of internal radius R_1 and external radius R_2, contains a circumferential crack of depth a from the external surface and is subjected to one of the following loading conditions:

(i) a uniform tensile stress σ applied remote from the crack and acting parallel to the tube axis (see Fig.154)

(ii) a uniform torque T applied, remote from the crack, about the tube axis (see Fig. 155).

This configuration was studied by Harris[8] for both conditions. He derived approximate expressions for the stress intensity factors from Neuber's[9] approximate stress concentration factors for notches.

For condition (i), the opening mode stress intensity factor is given by

$$\frac{K_I}{K_0}=\frac{1-N^2}{(1-(1-N)X)^2-N^2}\left\{0{\cdot}80+\frac{(1-N)X}{1-(1-N)X}\left[4+\frac{1{\cdot}08N}{(1-N)(1-X)}\right]\right\}^{-\frac{1}{2}} \quad (1)$$

where $N=R_1/R_2$ and $X=a/(R_2-R_1)$.

K_0 is given by

$$K_0=\sigma\sqrt{\pi a}\ . \quad (2)$$

Results calculated from equation (1) are shown in Fig.154 as curves of K_I/K_0 vs. $a/(R_2-R_1)$ for various values of R_1/R_2. For the case of a solid cylinder ($R_1/R_2=0$), Harris[9] compares his results with other approximate results and shows agreement to within a few per cent.

For condition (ii), the tearing mode stress intensity factor is given by

$$\frac{K_{III}}{K_0}=\frac{(1-N^4)(1-(1-N)X)}{(1-(1-N)X)^4-N^4}\left\{1+\frac{(1-N)X}{1-(1-N)X}\left[7{\cdot}111+\frac{2{\cdot}468N}{(1-N)(1-X)}\right]\right\}^{-\frac{1}{2}} \quad (3)$$

where K_0 is given by

$$K_0=\tau_m\sqrt{\pi a}\ , \quad (4)$$

where τ_m is the maximum shear stress which occurs at the outer surface of the tube and is given by

$$\tau_m=\frac{2R_2T}{\pi\left(R_2^4-R_1^4\right)}\ . \quad (5)$$

Results calculated from equation (3) are shown in Fig.155 as curves of K_{III}/K_0 vs. $a/(R_2-R_1)$ for various values of R_1/R_2. Wilson[10], using finite element techniques, obtained results for a long solid cylindrical bar under condition (ii) ($R_1/R_2=0$); his results agree, to within 5% with those shown in Fig.155.

EXHIBIT 19
Page 1 of 2

Compendium of Stress Intensity Factors
D.P. Rooke and D.J. Cartwright.
Discs, tubes and bars. pp 237-238

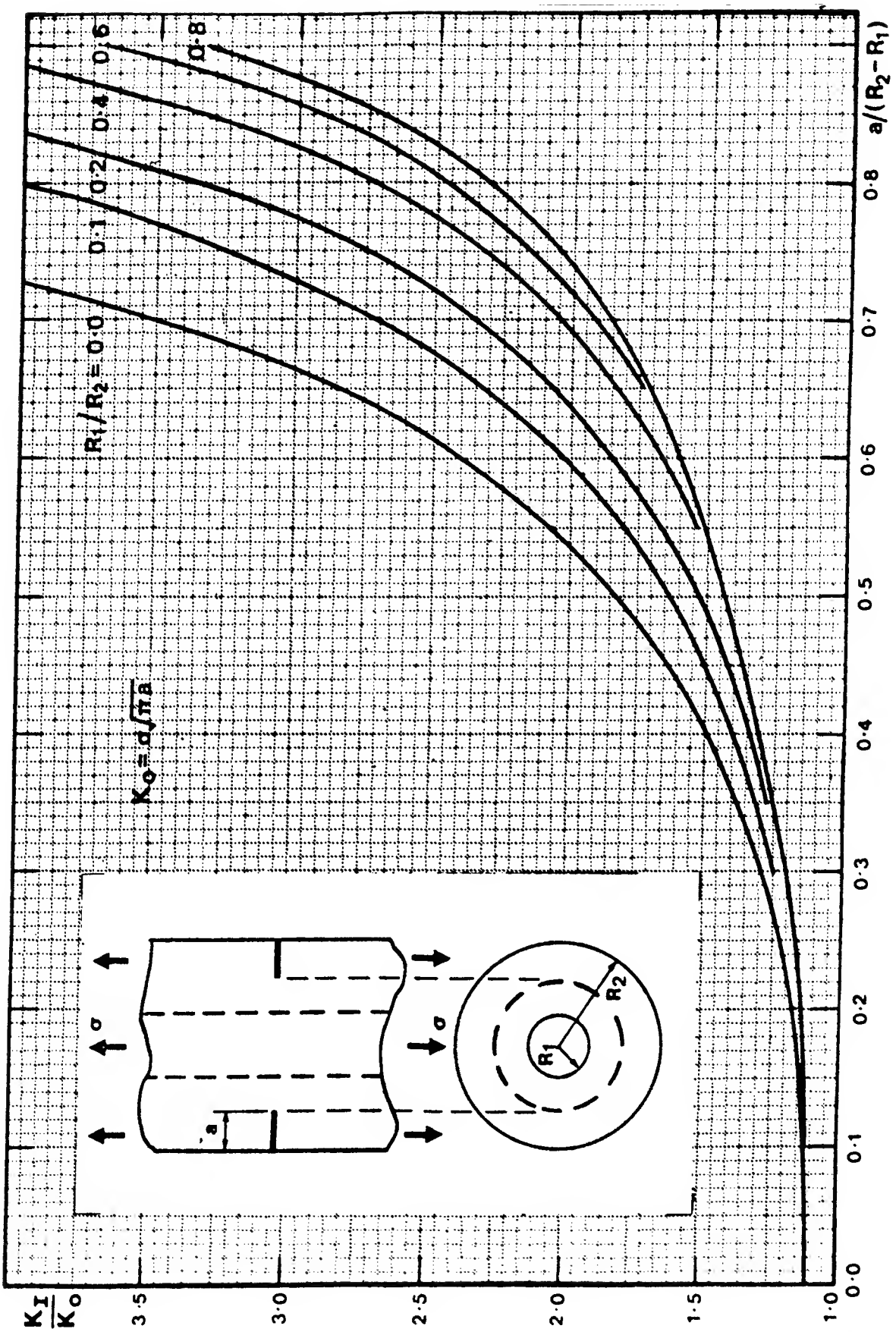

Fig. 154 K_I for an external circumferential crack in a tube subjected to a uniaxial tensile stress

EXHIBIT 19
Page 2 of 2

Odd number of collinear cracks in a sheet: uniform tensile stress or shear stress

A sheet containing an odd number (n) of cracks of length 2a periodically spaced a distance 2b apart is subjected to a uniform normal or shear stress remote from the crack (see Fig.93). Two conditions have been considered by Isida[40] using a perturbation technique:

(i) a uniaxial tensile stress σ perpendicular to the line of the cracks;

(ii) a shear stress τ parallel to the line of the cracks.

The results, which are accurate to within 1 %, for the central crack are shown in Fig.93 as curves of K_N/K_0 vs. a/b for various values of n, where K_0 is the stress intensity factor for an isolated ($b = \infty$) crack under the appropriate stress condition.

For condition (i),

$$K_N = K_I \quad (K_{II} = 0) , \tag{1}$$

and

$$K_0 = \sigma \sqrt{\pi a} , \tag{2}$$

for condition (ii),

$$K_N = K_{II} \quad (K_I = 0) , \tag{3}$$

and

$$K_0 = \tau \sqrt{\pi a} . \tag{4}$$

The case $n \to \infty$ has been studied by many workers [43,44,45,46] using various methods; the results are all in agreement. From the work of Westergaard[43] the following analytic expression can be derived;

$$\frac{K_N}{K_0} = \sqrt{\frac{2b}{\pi a} \tan\left(\frac{\pi a}{2b}\right)} . \tag{5}$$

All the above results are valid for the mode III stress intensity factor with

$$K_0 = \tau \sqrt{\pi a} , \tag{6}$$

where τ is the out-of-plane shear stress acting remote from the cracks, in a direction perpendicular to the cracked plane.

Compendium of Stress Intensity Factors
D.P. Rooke and D.J. Cartwright.
Flat sheets. pp 140-141

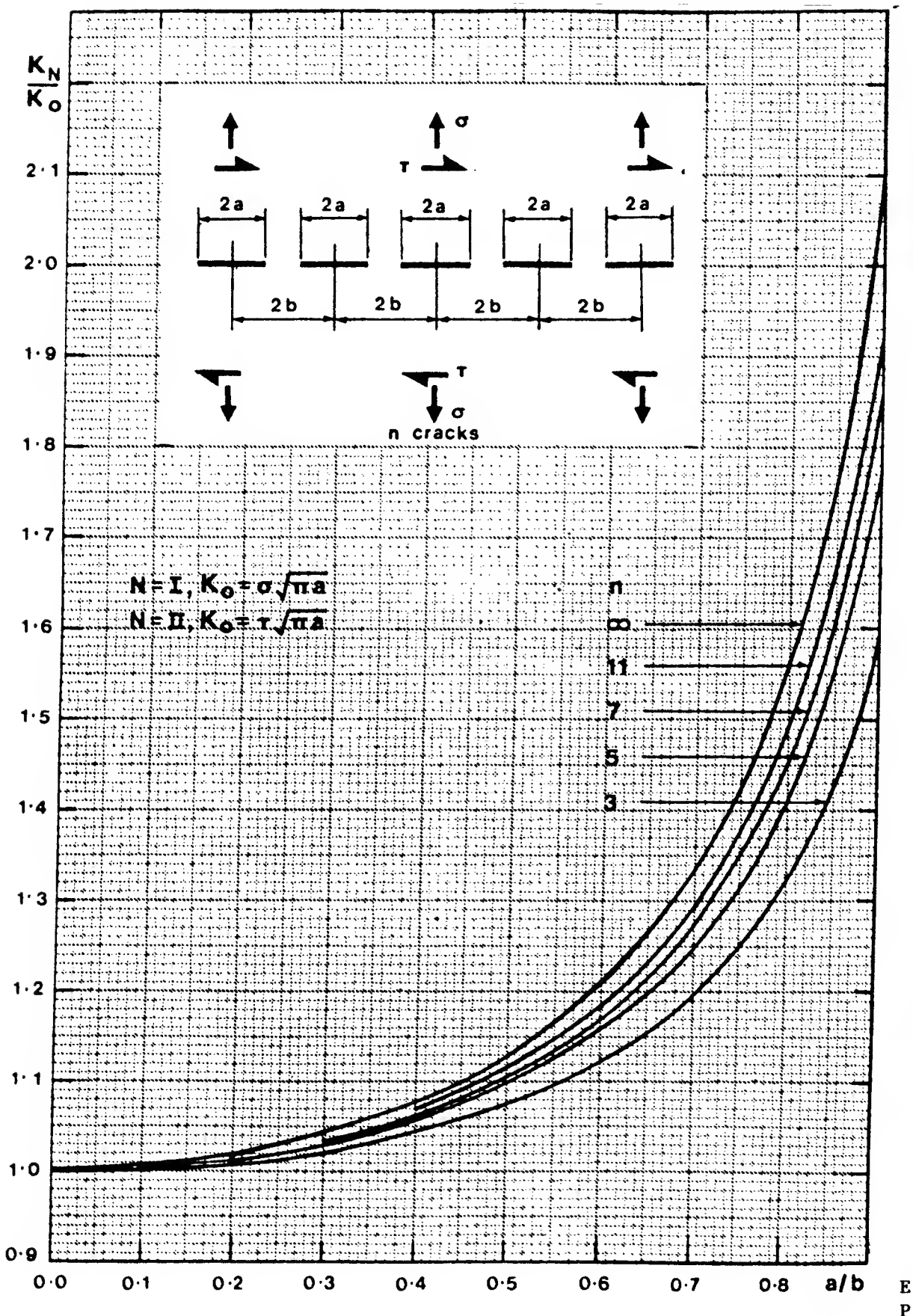

Fig.93 K_I and K_{II} for the central crack of n collinear cracks in a sheet subjected to a uniform normal or shear stress

Exhibit 21

FINITE THICKNESS CORRECTION FACTORS

This appendix summarizes the results obtained for the frontface and backface correction factors and their resultant, and compares them with the result obtained for the secant correction factor. The authors referenced were Shaw and Kobayashi[3], Smith and Sorensen[4], and Little and Bunting[5]. The flaw shape configuration examined was the circular/elliptical flaw. For all cases, the crack depth over thickness ratio, a/t, was taken as 0.77. The crack depth to crack length ratio, "a/2c" was examined for one fisheye, a cluster of fisheyes, and a string of contiguous fisheyes, i.e. a/2c equals 0.714, 0.303, and 0.0457, respectively.

FRONTFACE-BACKFACE CORRECTION FACTORS

SHAW AND KOBAYASHI[3]

Poissons's ratio = 0.30
b = crack depth
h = thickness
2a = crack length
M_k = combined frontface/backface correction factor
M_f = front face correction factor

Shaw and Kobayashi give the following equation for the calculation of the front face correction factor:

$M_f = 1.0 + 0.12\ (1\text{-}b/2a)$
$M_f = 1.0 + 0.12\ (1\text{-}0.0457)$
$M_f = 1.11$

M_k, the combined front and back face correction factors was obtained by the authors by multiplying the front and back face correction factors. Their interaction was not taken into account. The M_k value can be obtained directly from the curve shown in Figure 6.

a/2c = 0.714, b/a = 1.43, out of scale
a/2c = 0.303, b/a = 0.61, and M_k = 1.30
a/2c = 0.0457, b/a = 0.05, and M_k = 1.50

Note: b/a ratio > 1 corresponds to a circular flaw

SMITH AND SORENSEN[4]

Poisson's ratio = 0.25
M_k = combined front-back face correction factor

These authors considered the front and backface effects, as well as the interaction of the front and back faces. The M_k value can be obtained directly from the curve shown in Figure 7. On the same Figure, the curves obtained by Shah and Kobayashi are also shown for comparison. It can be seen that the stress intensity values are lower for Shah and Kobayashi. The curves corresponding to the a/2c ratio for a single fisheye and for a string of contiguous fisheyes, were not available.

a/2c = 0.3, M_k = 1.17
a/2c = 0.2, M_k = 1.30 (Kobayashi was 1.25)
a/2c = 0.2, M_k = 1.46 (Kobayashi was 1.35)

LITTLE AND BUNTING[5]

M_k = backface correction factor

Little and Bunting found that the backface correction factor was strongly material dependent, i.e. Poisson's ratio effect.

In the subject case, the material D6ac steel was considered since its Poisson's ratio is 0.30, similar to the subject sleeve material. the backface correction factor can be obtained directly from the curves shown in Figure 8. In this Figure, the effect of the Poisson's ratio can be readily seen.

for D6ac steel, 220 / 240 Ksi, a/2c = 0.09-0.12
$M_{backface}$ = 2.6

using M_{front} = 1.11 as per Shah and Kobayashi[3]

M_{total} = 2.6 x 1.11 = 2.9

SUMMARY FRONTFACE AND BACKFACE CORRECTION FACTORS

It is found that the most critical case is a slender elliptical or semi-elliptical flaw shape with a/2c less than 0.3, and a/t greater than 0.6, as opposed to a semi-circular or circular flaw shape. Knowing that the effect of the Poisson's ratio is to increase the correction factor, it was felt that the backface correction factor obtained by Little and Bunting for D6ac steel combined with the front face correction factor found using Shah and Kobayashi was more appropriate to the subject case. Thus,

M_{total} = 2.9.

SECANT CORRECTION FACTOR:

The secant correction factor[2] can replace accurately the polynomial expression used in finite width specimens. This correction is expressed as [secant (PI * a/W)]^{½}. In cases associated with a partial- through-thickness flaw, the width "W" is replaced by a quantity equals to twice the thickness dimensions, i.e. "2t".

Thus the fracture toughness expression becomes:

K= Sigma (PI * a)^{½} [sec (PI * a/2t)]^{½}

a = 0.0525 inch
2t = 2 * 0.068 inch = 0.1360 inch
[secant (PI * a/2t)]^{½} = cos - (1.2127 radians)
[secant (PI * a/2t)]^{½} = 1.69

SUMMARY

The frontface-backface correction factor with 2.9, is much greater than the finite width secant correction factor 1.69. For the purpose of our calculations, the worst of the two, i.e. the 2.9 frontface-backface correction factor, has been used.

EXHIBIT 22

FRACTURE TOUGHNESS AND THRESHOLD DATA

Given that our subject specimen had a UTS value of 195 Ksi, and had been tempered at 800°F for a period of 4 hours, the fracture toughness values under plane strain and plane stress conditions and the threshold values for stress corrosion cracking, and thin sheets were obtained from the literature and are summarized below.

TABLE 1

REF	UTS	YS	HRC	TEMP	THICK	K_I	K_{IC}	K_{ISCC}	K_{th}
6a	--	206	--	--	--	--	80	--	--
6b	240	--	--	--	--	--	--	--	35
7a	195	--	--	--	--	--	104	26	--
7b	--	--	--	800	--	80-100	--	--	--
8a	205	191	44	800	--	--	62	48	--
8b	--	--	--	800	--	--	65	27	--
8c	--	--	--	600	0.06	175	--	--	--
8c	--	--	--	600	0.4	--	65	--	--

UTS, YS are in Ksi units
Temper Temperature is in °F and thickness is in inches
K_I, K_{IC}, K_{ISCC}, K_{th} are in Ksi $\sqrt{inch}$

Reference 6a: Bend and compact specimens tested. (Page 47, Table 4.3)

Reference 6b: The threshold stress intensity for specimens of relatively thin sheets of steels, K_t, including 4340 steel, were subjected to sustained loading in an environment of distilled water. For thicker sheets in plane strain conditions, the threshold stress intensity would be the critical value of the stress corrosion cracking, K_{ISCC}, occurring at a significantly lower K value than for thin sheets. Our UTS being lower, at 195 Ksi, it is expected that the threshold value would be higher. (Pages 87, and page 90 Figure 4.42).

Reference 7a: K_{ISCC} for stress-corrosion cracking of plate in 3% aqueous sodium-chloride solution. (Code 1206, page 12, Table 2.0321)

Reference 7b: Effect of tempering temperature on range of fracture toughness.(Code 1206, page 26, Figure 3.02721)

Reference 8a: Comparison of properties between various steel alloys. Page 112.

Reference 8b: the ratio $K_{ISCC} / K_{IC} = 0.42$ was given,as well as the K_{ISCC} value. From these data, the value of K_{IC} was determined. Page 112.

Reference 8c: Graph at 6000°F temper, illustrating the influence of specimen thickness on the fracture toughness of 4340 steel. K_I is the plane stress fracture toughness value, and is 175 Ksi$\sqrt{inch}$ for a thickness of 0.40 inch. The values would be expected to be higher for a temper at 800°F. Page 127.

The tempering temperature, UTS and yield strength values, thickness and environment all have an effect on the fracture toughness and threshold values. As the tempering temperature is increased, the UTS and yield strength values will decrease, but the fracture toughness and the environmental threshold will increase. The yield strength is generally taken as 85 percent of the UTS value.

In summary, the following data will be used in the calculations.

K_I = 175 Ksi $\sqrt{inch}$
K_{IC} = 80 Ksi $\sqrt{inch}$
K_{ISCC} = 26 Ksi $\sqrt{inch}$
K_t = 35 Ksi $\sqrt{inch}$

FRACTURE MECHANICS AND HELICOPTER FAILURE (E)

SEMIELLIPTICAL/SEMICIRCULAR FLAW SHAPE

The case of the semielliptical/semicircular flaw shape is shown in Exhibit 17. Two cases were considered; first, the crack was exposed to the surface, and second, it was embedded into the material. The "Y" factor is 1.1 for a surface flaw and 1.0 for an embedded flaw.

An embedded elliptical or a semielliptical surface flaw will always grow to a circular shape, and as such, the ratio "a/2c"will increase to a limit value of 0.5 for the embedded elliptical flaw, and to a limit value of 0.36 for the semielliptical surface flaw. However, this applies if fatigue growth exists, and generally applies to a single crack. When several crack initiation sites are present (for example a cluster or string of either contiguous cracks or cracks which are very close to one another), and if fatigue growth becomes significant, they will blend together and behave as a single large flaw with decreasing "a/2c" ratio. In our case, very little fatigue growth had occurred, the hydrogen embrittlement fisheyes having been mostly dormant since the manufacturing process. Also, there were numerous crack initiation sites, mostly contiguous to one another. Therefore, I did not use the limit values of 0.5 or 0.36 for the calculations, but the actual "a/2c" ratios:

"a" = 0.0525 inches
"2c" = 0.0735 inches for the longest single fisheye
"2c" = 0.1732 inches for the longest cluster
"2c" = 1.15 inches for the longest string
"2c" = 14.23 inches for the entire sleeve perimeter

I considered four values for the fracture toughness:

K = 80 Ksi $\sqrt{}$inch, plane strain
K = 175 Ksi $\sqrt{}$inch, plane stress
K = 26 Ksi $\sqrt{}$inch, environmentally assisted cracking
K = 35 Ksi $\sqrt{}$inch, thin sheets

The general formula which applies for a semielliptical/semicircular flaw shape is:

$$K = M_k \, Y \, \sigma \, \sqrt{(\pi a/Q)}$$

where:

M_k = 2.9 for the frontface/backface correction factor
M_k = 1.69 for the secant correction factor
a = 0.0525"; maximum flaw depth observed

$K = 80, 175, 26 \text{ and } 35 \text{ Ksi } \sqrt{\text{inch}}$

The detailed calculations are found in Exhibit 23.

EXHIBIT 23

SOLUTION : SEMIELLIPTICAL/SEMICIRCULAR FLAW APPROACH

a) Evaluate the critical flaw size "a" for a semielliptical/semicircular flaw shape for:

1. fracture toughness data in plane strain, plane stress, environmentally assisted cracking and thin sheets;
2. for the secant correction factor and frontface/backface correction factor;
3. for a surface flaw and an embedded flaw

$a_{critical} = (K /(M_k Y \sigma))^2 (Q/\pi)$

a = 0.525 inches

K = 80 Ksi √inch plane strain fracture toughness
K = 175 ksi √inch plane stress fracture toughness
K = 26 Ksi √inch for environmentally assisted cracking
K = 35 Ksi √inch for thin sheets

M_k = 1.69 for the secant correction factor
M_k = 2.9 for the frontface/backface correction factor

Y = 1.0 for an embedded flaw
Y = 1.1 for a surface flaw

Flaw size "a/2c" and Q value:
"a" = 0.0525 inches
"2c" = 0.0735 inches for the longest single fisheye
"2c" = 0.1732 inches for the longest cluster
"2c" = 1.15 inches for the longest string
"2c" = 14.23 inches for the entire sleeve perimeter

Worst case calculation:

2c = 14.23 inches
a/2c = 0.004 and Q = 1, for σ / σ_y = 31.4 / 166 = 0.2
M_k = 2.9
K = 26 Ksi √inch
Y = 1.1 surface flaw

σ = 31.4 ksi

a critical = (K /(M_k Y σ))^2 (Q/π)
a = 0.021 inches

This flaw size (0.021 inches) is smaller than the flaw depth of 0.0525 inches, and therefore a flaw size of 0.0525 inches would be critical in environmentally assisted cracking conditions.

b) For which fracture toughness data is the flaw size most critical?

To find out the critical value of K :

K = M_k Y σ $\sqrt{(\pi a/Q)}$
K = 2.9 (1.1) 31.4 ksi $\sqrt{(\pi}$ 0.0525 inches/1)
K = 40 Ksi $\sqrt{}$inch

The fracture toughness value of 40 Ksi $\sqrt{}$inch is between the thin sheet fracture toughness data and the plane strain value of fracture toughness, but well above the environmentally assisted cracking fracture toughness.

c) Is a surface flaw a worse case than an embedded flaw?

The surface flaw is a worst case because the value of "Y" is 1.1 reducing the required depth of the critical flaw size.

FRACTURE MECHANICS AND HELICOPTER FAILURE (F)

THE CIRCUMFERENTIALLY CRACKED TUBE

The case of the circumferentially cracked tube flaw configuration is shown in Exhibit 19. For this case, the length of the crack is assumed to be the entire circumference, and the flaw depth the maximum depth observed considering all fisheyes, i.e. 0.0525 inches.

The case of a cracked tube subjected to uniaxial tensile stress has been reported by D.O. Harris[11]. The applicable curve is shown in Exhibit 19.

crack depth "a" = 0.0525 inch
wall thickness = 0.068 inch
sleeve outer diameter = 4.529 inches

The detailed calculations are found in Exhibit 24.

EXHIBIT 24

SOLUTION : EXTERNAL CIRCUMFERENTIAL CRACK IN A TUBE

a) Evaluate the critical stress intensity factor for the flaw shape configuration of a circumferentially cracked tube.

For this calculation, I considered two different values for the cracked area: the actual cracked area, i.e. 28%, and the cracked area corresponding to having the entire circumference as cracked. The reason behind this is that I wanted to use the same flaw depth of 0.0525 inches. If I had kept the same 28% area, I would have had to reduce this flaw depth to match the area.

Given a flaw depth of 0.0525 inches, I get a much greater cracked area, 77 percent, which gives me a new stress of 98 Ksi:

14,130 psi/0.23 = 61,435 psi
61,435 psi x 1.6 = 98,296 psi

The applicable graph is shown as Exhibit 19:

R_1 = internal radius = 2.187 inches
R_2 = external radius = 2.255 inches
a = crack depth = 0.0525 inch
K_I = stress intensity factor for opening mode

$R_1 / R_2 = 0.97$
$a / (R_2 - R_1) = 0.77$

for these values

$K_I / K_0 = 2.15$
$K_0 = \sigma \sqrt{(\pi a)}$
$K_I = 2.15 \sigma \sqrt{(\pi a)}$

where:

σ = 32 Ksi and 98 Ksi; loading stress
a = 0.0525 inches; maximum flaw depth observed

for σ = 32 Ksi:

$K_I = 2.15 \sigma \sqrt{(\pi a)}$
K_I = 2.15 (32 Ksi) $\sqrt{(\pi$ 0.0525")

K_I = 27.9 Ksi $\sqrt{inch}$

for σ = 98 Ksi:

$K_I = 2.15\ \sigma\ \sqrt{(\pi a)}$

$K_I = 2.15$ (98 Ksi) $\sqrt{(\pi\ 0.0525")}$

K_I = 85.6 Ksi $\sqrt{inch}$

Since the critical stress intensity factor for the higher stress, i.e. 98 Ksi was obtained by using a much greater percentage of cracked area, the value obtained at a stress value of 32 Ksi is considered more appropriate and will be used in further calculations.

b) Determine the effect of the frontface/backface correction factor on the value of the critical stress intensity factor using a stress value of 32 Ksi.

new $K = M_k \times K_I$

K = 2.9 x 27.9 Ksi $\sqrt{inch}$ = 81 Ksi $\sqrt{inch}$

This is very close to the plane strain fracture toughness value.

c) For which fracture toughness data: plane strain, plane stress, environmentally assisted cracking and thin sheets, is the stress intensity factor most critical?

For a stress of 32 Ksi, and considering a frontface/backface correction factor, it can be seen that the sleeve could fail under plane strain conditions.

d) Compare the critical stress intensity factor to the critical fracture toughness data found for the semielliptical/semicircular flaw shape ?

K semielliptical/semicircular flaw shape: 40 Ksi $\sqrt{inch}$.

K circumferentially cracked tube 81 Ksi $\sqrt{inch}$ (σ = 32 Ksi)

The circumferentially cracked tube is a more critical case than that of the semielliptical/semicircular flaw configuration.

FRACTURE MECHANICS AND HELICOPTER FAILURE (G)

MULTIPLE COLLINEAR EDGE CRACKS IN A SHEET

The case of the multiple collinear crack is shown in Exhibit 20. In this approach, the length of the crack was the average cluster size and the flaw depth the maximum depth observed considering all fisheyes, i.e. 0.0525 inches.

The effect of an odd number of collinear cracks in a sheet with uniform uniaxial tensile stress is shown in Exhibit 20[11].

There were approximately 48 clusters (each cluster including several individual fisheyes) along the entire circumference of the tube. On average, the length of a cluster was found to be:

$$2a = 0.1481 \text{ inch}$$

In one particular area, the clusters were all contiguous, which would make the periodic distance between them equal to the size of one cluster.

$$2b = 0.1481 \text{ inch}$$

At the limit, then, where the cracks contact each other, the ratio a/b will be 1.

$K_0 = s \sqrt{(\pi a)}$
a = 0.0525 inches; maximum flaw depth observed

The detailed calculations are found in Exhibit 25.

EXHIBIT 25

SOLUTION : ODD NUMBER OF COLLINEAR CRACKS IN A SHEET

a) Evaluate the critical stress intensity factor for the given flaw depth.

2a = 0.1481 inch (length of cluster)
2b = 0.1481 inch (distance between clusters)
a/b = 1

The curves for a total of 11 cracks and an infinite number of cracks are very close to each other, and, since the number of clusters was more than 11, the curve for an infinite number of cracks will be used.

The ratio a/b = 0.9 will be used since the ratio 1.0 is not available in Exhibit 20, and cannot be extrapolated, as the curve for an infinite number of cracks is divergent for a/b = 0.9.

For these values:

$K_N / K_0 = 2.10$
$K_0 = \sigma \sqrt{(\pi a)}$
$K_N = 2.10\ \sigma \sqrt{(\pi a)}$

where:

σ = 32 Ksi ; loading stress
a = 0.0525 inches; maximum flaw depth observed

$K_N = 2.10 \times 32$ Ksi $\sqrt{(\pi\ 0.0525}$ inch)
$K_N = 27.3$ Ksi $\sqrt{}$inch

The critical stress intensity factor was found to be 27.3 Ksi $\sqrt{}$inch.

b) Determine the effect of the frontface/backface correction factor on the value of the critical stress intensity factor.

new $K = M_k \times K_I$

K = 2.9 x 27.3 Ksi $\sqrt{}$inch = 79 Ksi $\sqrt{}$inch

This is very close to the plane strain fracture toughness value.

c) For which fracture toughness data: plane strain, plane stress, environmentally assisted cracking and thin sheets, is the stress intensity factor most critical?

For a stress of 32 Ksi, and considering a frontface/backface correction factor, it can be seen that the sleeve could fail under plane strain conditions.

d) Compare the critical stress intensity factor for the collinear edge cracks to that found for the circumferentially cracked tube and the critical fracture toughness data for the semielliptical/semicircular flaw shape ?

K semielliptical/semicircular flaw shape: 40 Ksi $\sqrt{inch}$.

K circumferentially cracked tube 81 Ksi $\sqrt{inch}$ (σ = 32 Ksi)

K collinear edge cracks 79 Ksi $\sqrt{inch}$ (σ = 32 Ksi)

The odd number of collinear cracks in a sheet is similar to the circumferentially cracked tube, and both are more critical cases than the semielliptical/semicircular approach.

FRACTURE MECHANICS AND HELICOPTER FAILURE (H)

COMPARING THE FLAW CONFIGURATIONS

An evaluation of the data obtained from the calculations carried out for the three different flaw configurations is necessary to evaluate the fracture toughness/stress intensity factor value.

The critical values obtained for fracture toughness/stress intensity factors using a stress of 32 Ksi, a flaw depth "a" = 0.0525 inches, a frontface/backface correction factor of 2.9 and a surface flaw (Y = 1.1) were:

K semielliptical/semicircular shape = 40 Ksi $\sqrt{inch}$.

K circumferentially cracked tube = 81 Ksi $\sqrt{inch}$

K odd number of collinear cracks in a sheet = 79 Ksi $\sqrt{inch}$

These values indicated that for the semielliptical/semicircular flaw shape, environmentally assisted cracking conditions had to exist for the flaw depth 0.0525 inches to be critical.

However, several facts indicated that environmentally assisted cracking conditions did not exist:

- the cracks were dormant, and fatigue had progressed only slightly from the fisheyes;
- the tensile test clearly showed that under sustained loading approaching 100% of the yield stress, the material did not fail;
- with the exception of one coupon out of eight, the average UTS value was within the required manufacturer's specifications of 195 Ksi;
- the fractographic features were consistent with plane stress conditions;
- the only other known sleeve failure had occurred under normal operating loading conditions, but its precracking was greater and involved significant fatigue growth.

As for the Edmonton sleeve, the flaws in the Omanian sleeve initiated due to hydrogen embrittlement, and progressive cracking was in a fatigue mode, not in an intergranular mode. If the Edmonton sleeve had been in an embrittled condition, an intergranular type of progressive failure would not have been observed.

Now, looking at the cases of the circumferentially cracked tube and odd number of collinear cracks, plane strain conditions had to exist for the flaw depth 0.0525 inches to be critical. A significant difference existed in the results between these two cases and that of the semielliptical/semicircular flaw. Possibly the flaw size conditions which had been considered represented much worse conditions than those actually present. Now that I had accumulated significant data and understanding in this problem, I could re-examine the data from the Omanian sleeve and re-evaluate the flaw configurations.

But first, I wanted to get an idea of the critical flaw size for the three flaw configurations I had considered using the plane strain value of fracture toughness 80 Ksi $\sqrt{\text{inch}}$. These are detailed in Exhibit 26.

EXHIBIT 26

SOLUTION: COMPARING THE FLAW CONFIGURATIONS

a) Using the value of plane strain fracture toughness, 80 Ksi √inch, evaluate the critical flaw size for the flaw configurations previously considered, and draw conclusions.

the semielliptical/semicircular flaw
the circumferentially cracked tube
the multiple collinear cracks in a sheet

SOLUTION:

the semielliptical/semicircular flaw

$$a_{critical} = (K / (M_k Y \sigma))^2 (Q/\pi)$$
$$a = (80 \text{ Ksi } \sqrt{\text{inch}} /(2.9 \times 1.1 \times 32 \text{ Ksi}))^2 (1/\pi)$$
$$a = 0.195 \text{ inches}$$

The critical flaw size is 3 times the thickness of the sleeve (0.068 inches).

the circumferentially cracked tube

$$K_I = 2.15 \sigma \sqrt{(\pi a)}$$
$$a = (K_I / (M_k 2.15 \sigma))^2 1/ \pi$$

$$a = (80 \text{ Ksi } \sqrt{\text{inch}} / (2.9)(2.15 \times 32 \text{ Ksi}))^2 1/\pi$$

$$a = 0.051 \text{ inch}$$

The critical flaw size is 0.75 times the thickness of the sleeve (0.068 inches).

the multiple collinear cracks in a sheet

$$K_N = 2.10 \sigma \sqrt{(\pi a)}$$
$$a = (K_N / (M_k 2.10 \sigma))^2 1/ \pi$$

$$a = (80 \text{ Ksi } \sqrt{\text{inch}} / ((2.9) 2.10 \times 32 \text{ Ksi}))^2 1/ \pi$$
$$a = 0.054 \text{ inch}$$

The critical flaw size is 0.79 times the thickness of the sleeve (0.068 inches).

It is quite obvious that when the plane strain value of fracture toughness is used for the

different flaw configurations, the sleeve will not fail under normal loading conditions for the semielliptical/semicircular flaw but will fail for the circumferentially cracked tube and the multiple collinear cracks in a sheet.

FRACTURE MECHANICS AND HELICOPTER FAILURE (I)

FRACTURE TOUGHNESS AND FLAW SIZE FROM OMANIAN SLEEVE

In my "ball-park" figure calculation for the fracture toughness on the Omanian sleeve, I had not considered the frontface/backface correction factor M_k of 2.9, nor the secant correction factor 1.69, and the fracture toughness value obtained was rather low at 56 Ksi √inch. By considering these factors, how close would I get to the "Battelle Structural Alloys Handbook"[8] plane strain and plane stress values of fracture toughness, 80 Ksi √inch and 175 Ksi √inch, respectively. I knew from the conditions observed for the sleeve that it was most likely that either plane strain or plane stress conditions existed.

And if the plane strain and plane stress values of fracture toughness are considered, what was the critical flaw size ? Was it close to what was actually observed on the Omanian sleeve ?

What flaw configuration best correlated to these findings: the semielliptical/semicircular flaw, the circumferential cracked tube flaw or the odd number of collinear cracks in a sheet ?

I carried out these calculations, and the results are shown in Exhibit 27.

I now had a much better picture of what the true fracture toughness value was as well as the most appropriate flaw configuration.

EXHIBIT 27

SOLUTION : FRACTURE TOUGHNESS FROM OMANIAN SLEEVE

a) Compare the value of the fracture toughness derived from the "ball-park" calculations for the Omanian sleeve to that obtained when the frontface/backface correction factor is taken into account. How close is this to the values obtained from the "Structural Alloys Handbook" by Battelle Institute.

$$K = M_k \, Y \, \sigma \, \sqrt{(\pi \, a \, / \, Q)}$$
$$K = 2.9 \times 1.1 \times 122.6 \text{ Ksi } \sqrt{(\pi \, 0.050 \text{ inch} \, / \, 0.9)}$$
$$K = 163 \text{ Ksi } \sqrt{\text{inch}}$$

This value is equivalent to 56 ksi $\sqrt{\text{inch}}$ previously found when no frontface/backface correction factor is taken into account.

The value of 163 Ksi $\sqrt{\text{inch}}$ is very close to the value of plane stress fracture toughness obtained from the "Structural Alloys Handbook" by Battelle Institute, 175 Ksi $\sqrt{\text{inch}}$.

b) Evaluate the critical flaw size for the Omanian sleeve when using the value of plane stress fracture toughness 175 Ksi $\sqrt{\text{inch}}$ and the frontface/backface correction factor.

$$\text{"a" critical} = (K \, / \, (M_k \, Y \, \sigma))^2 \, (Q/\pi)$$

$$a = (175 \text{ Ksi } \sqrt{\text{inch}} \, / \, (\, 2.9 \times 1.1 \times 122.6 \text{ Ksi}) \,)^2 \, (0.9 \, / \pi)$$
$$a = 0.057 \text{ inches}$$

This value is very close to what was actually observed on the Omanian sleeve, i.e. a crack depth varying from 0.050 to 0.060 inches.

c) The fact that the critical flaw size is what was actually found on the Omanian sleeve indicates that a good correlation exists between the variables chosen for the calculations and the actual conditions for the failed sleeve. These variables are : the semielliptical/semicircular flaw configuration, the plane stress fracture toughness, the surface flaw approach (Y = 1.1) and the 32 Ksi stress applied.

FRACTURE MECHANICS AND HELICOPTER FAILURE (J)

CRITICAL FRACTURE TOUGHNESS AND STRESS FOR OUR SLEEVE

From the revised calculations for fracture toughness on the Omanian sleeve, the value of plane stress fracture toughness in a semielliptical/semicircular flaw configuration appears to be the closest to the conditions actually observed for the Omanian sleeve. Other operational factors which could have affected the sleeve, were not considered significantly different between the Omanian sleeve and our Edmonton sleeve.

What would be the critical flaw size for our sleeve when using the value of plane stress fracture toughness 175 Ksi $\sqrt{\text{inch}}$ and the frontface/backface correction factor ?

How does this compare with the value obtained in the "ball-park" calculations ?

If we assumed that our flaw size was critical what would be the critical stress for failure and to what extent of precracking did this value correspond ? The results of these calculations are shown in Exhibit 28.

EXHIBIT 28

SOLUTION : FRACTURE TOUGHNESS FOR THE EDMONTON SLEEVE

a) Evaluate the critical flaw size for our sleeve when using the value of plane stress fracture toughness 175 Ksi √inch and the frontface/backface correction factor, and compare the value to that found in the ball-park calculations.

$$\text{"a" critical} = (K / (M_k Y \sigma))^2 (Q/\pi)$$

$$a = (175 \text{ Ksi } \sqrt{\text{inch}} / (2.9 \times 1.1 \times 32 \text{ Ksi}))^2 (1/\pi)$$
$$a = 0.936 \text{ inches}$$

This value is very close to that obtained for the "ball-park" figure, i.e. 0.84 inches.

b) Evaluate the critical stress value for failure and the extent of precracking which would be required to reach that stress.

$$\sigma = K / (M_k Y) \sqrt{(Q/(\pi a))}$$

$$\sigma = 175 \text{ Ksi } \sqrt{\text{inch}} / (2.9 \times 1.1) \sqrt{(1/(\pi\ 0.0525 \text{ inches}))}$$
$$\sigma = 135 \text{ Ksi}$$

This corresponds to a total fractured area of :

$$135 \text{ Ksi} \times \% \text{ area still holding} = 22.6 \text{ Ksi}$$
$$\text{area still holding} = 0.167 \%$$

Therefore the sleeve must be 83% cracked before critical conditions for failure are achieved.

FRACTURE MECHANICS AND HELICOPTER FAILURE (K)

CONCLUSIONS

Based on the Omanian sleeve data, and considering that both sleeves were subject to similar operating conditions, a value of plane stress fracture toughness of 175 Ksi √inch and a semielliptical/semicircular flaw configuration seem to be most appropriate for the final fracture mechanics evaluation of the Edmonton sleeve. Excellent correlation was found between the Omanian sleeve and our sleeve.

The calculations showed that with only 28 percent of the load bearing area cracked, and under maximum normal loading conditions, the sleeve could only fail if the fracture toughness was associated with environmentally assisted cracking conditions. However, the evidence showed that the sleeve did not fail while under environmentally assisted cracking conditions, but rather suggested that the fracture occurred in fully plane stress condition.

The fracture mechanics calculations showed that 83 percent of the sleeve cross-section would have to be cracked with maximum in-flight service loads before failure occurred. The Omanian sleeve had been precracked approximately 85 percent and broke under normal loading conditions. This indicated that for our sleeve, the loads applied at the time of failure were well in excess of the maximum in-flight loads that the sleeve would see during normal service. Thus, indicating that "mast bumping" likely caused the overstress which failed the sleeve. The Omanian sleeve failed after only 123.4 hours service, while the critical flaw size for our sleeve had not been reached when the accident occurred at 2039 hours.

After doing all these calculations, I found that the original "ball-park" figure of 0.84 inches for the critical flaw size was not so far off. For that rough calculation, I had used "Q = 1", and a fracture toughness value of 56 Ksi √inch as determined from the "ball-park" calculations on the Omanian sleeve. If you consider the plane stress fracture toughness of 175 Ksi √inch and the frontface/backface correction factor, you get a value of 0.936 inches, approximately 10 percent off from the "ball-park" figure.

During the course of this investigation, BHT replaced all collective sleeves manufactured in that particular batch, for the aircraft still in service. Further, on February 2nd, 1986, the aircraft manufacturer issued Service Bulletin 214ST-86-33 which replaced the collective sleeve part number 214-010-411-001/-003 by a new sleeve, part number 214-010-411-111. This new sleeve had increased shot peening coverage and was coated with tungsten carbide instead of chromium plating (Exhibit 29).

The report I wrote on the Fracture Mechanics calculations was only one of a total of 15 separate engineering reports produced by the Transportation Safety Board of Canada. The results of these reports were included into the final accident report submitted by the Chief investigator of the accident.

The final report concluded that mast bumping during flight was the lead event into the in-flight break-up and subsequent crash.

ECL-283 (K)
Exhibit 29

ALERT SERVICE BULLETIN NO. 214ST-86-33

Bell Helicopter TEXTRON
A Subsidiary of Textron Inc.

DATE 2-20-86

REV

P.O. Box 482 • Fort Worth, Texas 76101

PAGE NO. 1 of 3

MODEL AFFECTED: 214ST

SUBJECT: COLLECTIVE SLEEVE ASSEMBLY, P/N 214-010-411-001/-003, INTRODUCTION OF

HELICOPTERS AFFECTED: 214ST S/N's 28101 through 28150.

[214ST S/N 28151 and subsequent and spares shipped after 31 January 1986 will comply with this bulletin prior to delivery.

COMPLIANCE: On or before 30 April 1986

This bulletin cancels and supersedes A.S.B. 214ST-85-30.

DESCRIPTION:

A new collective sleeve assembly, P/N 214-010-411-111, has been developed which has increased shot peening coverage and is coated with Tungsten carbide in lieu of chrominum plating.

The purpose of this bulletin is to require that on or before 30 April 1986, all installed and spare collective sleeve assemblies, P/N 214-010-411-001/-003, be replaced with sleeve assembly, P/N 214-010-411-111. The retirement life for the new sleeve assembly is 5,000 hours.

FAA APPROVAL:

The Design Engineering aspects of this bulletin are FAA approved.

MANPOWER:

It is estimated that eight (8) man-hours may be required to accomplish this bulletin. Man-hours are based on "Hands On" time. Elapsed time to accomplish required task may vary due to manpower and facilities available.

A.S.B. 214ST-86-33
Page 2 of 3

WARRANTY:

Material required to comply with this bulletin should be ordered through your normal BHTI supply source. Operators are eligible for 100% warranty credit for parts used to comply with this bulletin. To apply for this special credit operators must submit a completed DMR requesting warranty per current BHTI warranty procedures. Collective sleeves removed from service must be returned with a copy of the DMR to:

Bell Helicopter Textron Inc.
Logistics Center
Trinity Blvd. and Norwood
Ft. Worth, Texas 76107
Attention: CPR Monitor

MATERIALS:

The following part is required to accomplish this bulletin and can be purchased at your normal BHTI Spare Parts Outlet.

Part Number	Nomenclature	Quantity
214-010-411-111	Sleeve, Collective	1 ea.

WEIGHT AND BALANCE:

Not affected

ELECTRICAL LOAD DATA:

Not affected

REFERENCES:

214ST Maintenance Manual Chapters 62-01-00 and 62-21-00.
214ST Component Repair and Overhaul Manual, Chapter 62-21-05 through 62-21-09.

PUBLICATIONS AFFECTED:

214ST Illustrated Parts Breakdown Chapter 62-21-00, Figure 3.
214ST Maintenance Manual, Chapter 4-00-00.

ACCOMPLISHMENT INSTRUCTIONS:

1. Remove main rotor hub and blade assembly, and pitch links in accordance with the Maintenance Manual, Chapter 62-01-00. Using the Maintenance and Component Repair and Overhaul Manuals, disassemble and/or remove only the parts required to replace the collective sleeve.

a. For removal, inspection and installation instruction for the scissors and sleeve assembly, refer to the Maintenance Manual, Chapter 62-21-00.

b. For disassembly and assembly instructions for the scissors and sleeve assembly, refer to the Component Repair and Overhaul Manual, Chapters 62-21-05 through 62-21-09.

2. Reinstall pitch links and hub and blade assembly in accordance with Chapter 62-01-00.

3. Record bulletin compliance in Helicopter Historical Service Record (Form 7861-56717 Rev. 483).

FRACTURE MECHANICS AND HELICOPTER FAILURE

Instructors Notes

Prepared by G.Kardos

This case history describes the approach necessary to carry out a thorough Fracture Mechanics investigation into the failure of an helicopter component. The analysis is eventually complicated by the requirement to prove a negative. That the component under investigation was not the cause of failure, although it was suspect.

The details of the investigation are related by Ms. Diane Rocheleau. She had worked for three years in the field of failure analysis and accident investigation for the Transportation Safety Board of Canada (TSBC). The Case is based upon an Independent Study submitted by Ms. Rocheleau towards completion of her Masters Degree in Mechanical Engineering at Carleton University in Ottawa, Canada.

Ms. Rocheleau describes the sequence of her fracture mechanics calculations on a helicopter collective sleeve which had failed in flight. The purpose of the calculations was to determine whether the sleeve failure was the lead event in the accident. The project tried her experience as a failure analyst and Fracture Mechanics.

The case study has been divided into a number of parts. The purpose for doing this is so that students can be guided through the analysis. Each part can be assigned for study or home work in turn. Their solutions can be compared with those of Ms. Rocheleau. Alternately the entire case can be studied to show how Fracture Analysis is applied in real problems.

Some of the questions that Students can asked to deal with are as follows:

Part (A)

This part gives the details of accident, and the component that may have caused the failure. Students can be asked what should be done toward the solution.

Diane saw her immediate tasks be to:

a) determine if possible the fracture toughness properties from the plastic zone size;

b) determine if plane strain or plane stress conditions existed

c) determine the fracture toughness from the Omanian sleeve failure; since this sleeve was known to have failed under normal operating conditions, the flaw size had reached critical dimensions;

d) estimate the critical flaw size on our sleeve, and compare it to the deepest flaw size observed.

Students could be asked to make these determinations.

Part B
This section can be used as a discussion of Diane's solutions and her "Ball-Park" solutions. How useful are "Ball-Park" solutions. What conclusions can be made about the failure? Are they valid? How good are they for the purpose?

Part C
Here Diane is given further information about possible causes of the accident. In the light of this students can be asked to discuss how they would go about getting a more definitive answer.

Part D
In this part Diane presents her steps to getting a more accurate Fracture Mechanics analysis of the failed sleeve.

Diane saw her immediate steps to be: "First I will start with the semielliptical/semicircular flaw shape (Exhibit 17), and determine the following:

a) using the four fracture toughness data, i.e., plane strain, plane stress, environmentally assisted cracking and thin sheets, and taking into account the secant correction factor and frontface/backface correction factor determine the critical flaw size in each case;

b) compare the data to find the critical fracture toughness value for our flaw size and determine which fracture toughness condition corresponds to this critical value;

c) compare the results for a surface flaw and an embedded flaw, and find out which is the worst case."

Once more after suitable discussion students could be asked to carry out these computations

Part E:
Diane at the completion of tasks in Part E defines the next steps as: "I now considered my second flaw configuration, the circumferentially cracked tube (Exhibit 19), and determined the following:

a) the critical stress intensity factor;

b) the effect of the frontface/backface correction factor on the value of the critical stress intensity factor;

c) comparison of this data to the fracture toughness data being considered : plane strain, plane stress, environmentally assisted cracking and thin sheets, and determine for which fracture toughness condition data the flaw size "a" is most critical;

d) comparison the results with those obtained for the previous flaw configuration: the semielliptical/semicircular flaw shape."

Part F

At the end of Part Diane decided to consider a third flaw configuration, the multiple collinear edge cracks in a sheet (Exhibit 20), and determined the following:

a) evaluate the critical stress intensity factor;

b) determine the effect of the frontface/backface correction factor on the value of the critical stress intensity factor;

c) compare this data to the fracture toughness data being considered : plane strain, plane stress, environmentally assisted cracking and thin sheets, and determine for which fracture toughness data the flaw size "a" is most critical;

d) compare the results with those obtained for the previous two flaw configurations: the semielliptical/semicircular flaw shape, and the circumferentially cracked tube;"

Part G

At this stage, students like Diane should look at what has gone before to see where to go next.

"I had now considered several flaw configurations and obtained different critical values of fracture toughness and stress intensity factors. An evaluation of this data and what it meant was the next step. I should consider which of the fracture toughness and stress intensity factors was most critical and evaluate if the conditions for that particular case were actually present when the sleeve failed. From this I could establish a conservative value of fracture toughness and use it in my final determination of the critical flaw size for all three flaw configurations considered.

I should consider the following factors :

- macroscopic and microscopic fracture features;
- flaw size;
- results from the various tests conducted;
- environmental operating conditions;

- known other previous failures"

Part H

At this point Diane suggest a way to confirm and legitimize her results: "Now I could go back and look at the Omanian sleeve data once more, and determine the effect of the frontface/backface correction factor and the secant correction factor. This would also help me evaluate the best of the three flaw configurations. Also, from the new value of fracture toughness found, I could go back and find the critical flaw size for the Omanian sleeve and compare it to the actual flaw size."

Part I

"I now had a much better picture of what the true fracture toughness value was as well as the most appropriate flaw configuration. and I could apply these to our sleeve and calculate the critical stress and flaw size."

Part J

All the computations are now complete. But still decisions have to be made. What do the computations reveal? What do they say about the failure of the sleeve and the cause of the accident? Now comes the important part of any project, the evaluation and recommendations. These questions and the discussion by the class of the results and conclusions in Part K reveal the purpose of 250 hours of investigation.